

## Anyui Volcano in Chukotka: Age, Structure, Peculiarities of Rocks' Composition and Eruptions

M. M. Pevzner<sup>a,\*</sup>, D. O. Gertsev<sup>a,†</sup>, P. I. Fedorov<sup>a</sup>, F. A. Romanenko<sup>b</sup>, and Yu. V. Kushcheva<sup>a</sup>

<sup>a</sup>*Geological Institute, Russian Academy of Sciences, Moscow, 11901 Russia*

<sup>b</sup>*Faculty of Geography, Moscow State University, Moscow, 119991 Russia*

\**e-mail: m\_pevzner@mail.ru*

Received March 9, 2016

**Abstract**—The study of lavas and pyroclastics from Anyui Volcano made it possible to reconstruct succession of its eruption events. The age of the eruption is estimated by isotopic methods to be  $0.248 \pm 0.030$  Ma. It is established that the last episode of volcanic activity in northeastern Russia occurred 0.2–0.5 Ma ago (in its continental part, 0.2–0.3 Ma ago). This episode is chronologically close to the last peak in activation of volcanism in the Arctic and Subarctic regions. The absence of features indicating glacial influence on lavas from Anyui Volcano provides grounds for an assumption that no significant glaciations took place in the continental areas of western Chukotka during the last 250 ka.

DOI: 10.1134/S0024490217010059

Anyui Volcano located in the continental part of western Chukotka is known since 1952, when it was discovered during the aerial photography. The intraplate position and extremely fresh appearance of lavas attracted immediately particular attention of geologists to this structure. Nevertheless, age of the volcano and the type of its eruption remain debatable. The volcano is known under different names: Anyui, Monni, Molydykh, and Ustiev. The first information on this structure was provided by E.K. Ustiev, who traced its integral lava flow (56 km) up to the cinder cone and described in detail this unique structure of Chukotka in 1953 (Ustiev, 1959). Precisely, this researcher described it as Anyui Volcano and we also prefer to use this name.

In 2009, we visited Anyui Volcano with the main purpose to determine the age of its eruption. To achieve the goal, we reconstructed the succession of eruptions of individual lava portions in addition to radiometric dating. In this article, we consider in detail different aspects of performed geochronological investigations, type of eruptive activity, and succession of different eruption phases. In addition, we analyze most of available published data on the composition of lavas and pyroclastics of Anyui Volcano, which allows main peculiar features of magmatic activity of this eruption to be characterized.

### TECTONIC POSITION

Anyui Volcano ( $67^{\circ}10'27''$  N,  $165^{\circ}50'08''$  E, 1054 m) is located in the Bol'shoi Anyui River basin at the head

<sup>†</sup> Deceased.

of the Monni River (“Rocky River”). Its cinder cone is confined to the northern slope of Mount Vulkanaya (1585 m), one of the highest peaks of the South Anyui Range. Anyui Volcano is an element of the synonymous group, which also includes the Aluchin and Bilibin volcanoes (Fig. 1, inset). The Anyui group of volcanoes is located in the western part of Chukotka within the South Anyui suture and near the Okhotsk–Chukotka volcanic belt (Korago et al., 2010; Sokolov et al., 2010) (Fig. 1, inset). The suture inherits the southern boundary of the Arctida paleocontinent (Laverov et al., 2013) and is located at the junction of the North America, Eurasia, and Sea of Okhotsk plates (Mazarovitch and Sokolov, 2003; Khain et al., 2009; Korago et al., 2010; Sokolov et al., 2010; Laverov et al., 2013).

The study area is located in the region with a distinct low-velocity seismic anomaly in the upper mantle, which may be determined as the asthenospheric rise of a mantle plume (Yakovlev et al., 2012; Dobretsov et al., 2013; Vernikovskii et al., 2013). During the Pliocene–Quaternary, volcanic activity in northeastern Russia was relatively low (Imaev et al., 1998; Akinin et al., 2008). Moreover, most of the known indications of volcanic activity of that time are localized near boundaries of plates with high seismic activity, while the Anyui group of volcanoes occupies the intraplate position (Fig. 1).

The cinder cone of Anyui Volcano crowns the Early Cretaceous large intrusion (Mount Vulkanaya), which is surrounded by Lower Triassic sedimentary rocks (Fig. 2). According to the U–Pb (SHRIMP-RG) dating, granitoids of Mount Vulkanaya are  $108.5 \pm 2.7$  Ma old (Miller et al., 2009). In

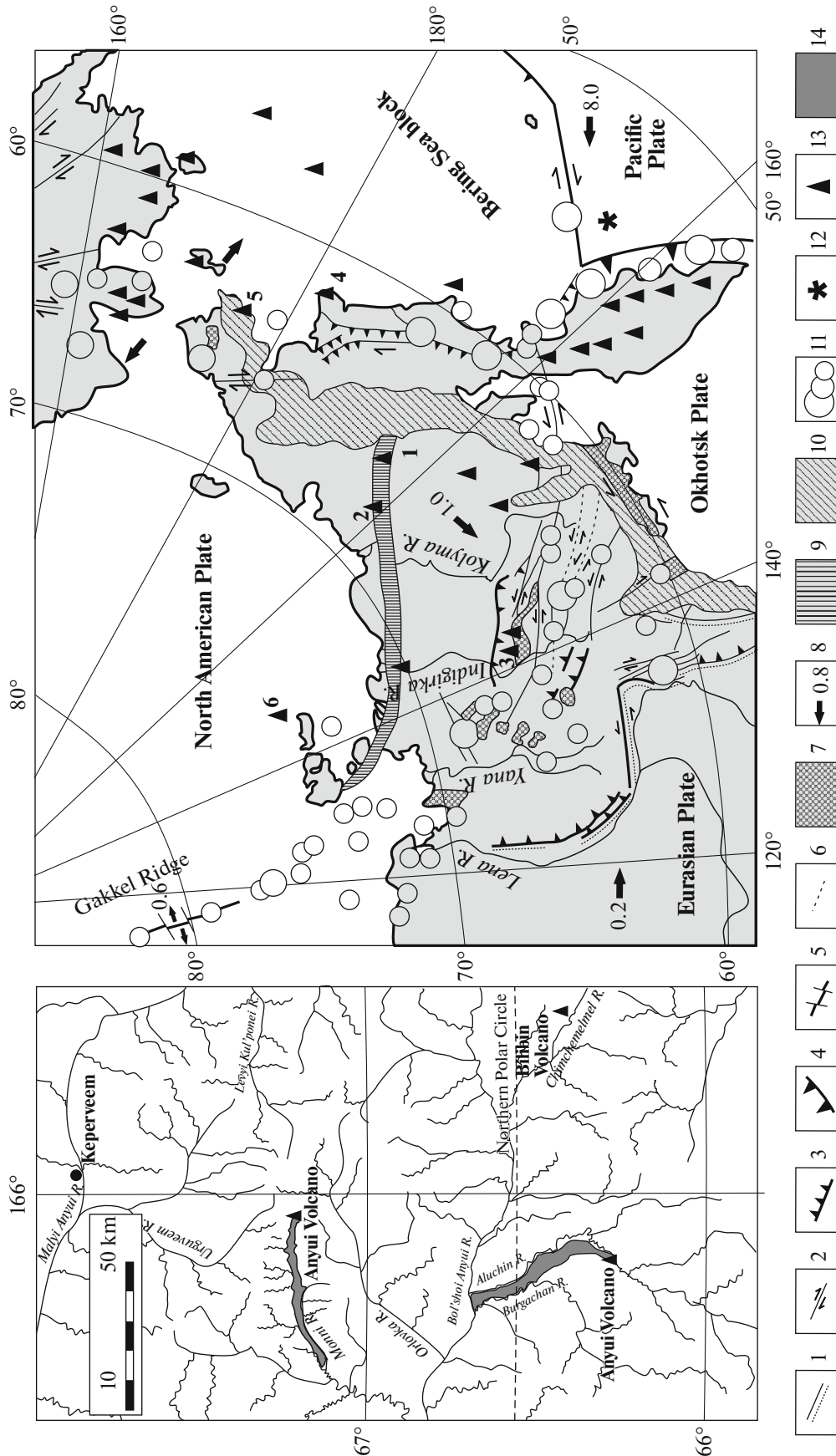


**Fig. 1.** Centers of Neogene–Quaternary volcanism in northeastern Asia and Alaska in the context of recent geodynamics (Imaev et al., 1998), modified after (Akinin et al., 2008; Korago et al., 2010; Vermikovskii et al., 2013). In the inset, location of volcanoes of the Anyui group. (1–3) active faults: (1) normal, (2) strike-slip, (3) thrusts; (4) boundaries of the subduction zone; (5) spreading zone of the Gakkel Ridge; (6) passive faults; (7) Cenozoic depressions; (8) direction and velocity of motions of individual plates and blocks; (9) South Anyui suture; (10) Okhotsk–Chukotka volcanic belt; (11) epicenters of earthquakes with the magnitude of  $>7.0$ ,  $6.0–6.9$ , and  $<6.0$ ; (12) location of ODP Hole 883 (Prueher and Rea, 2001); (13) Miocene–Quaternary volcanic centers; (14) fields of lava flows. Numerals: (1) Anyui group of volcanoes, (2) Pyatistennyi Volcano, (3) Balagan Tas Volcano, (4) volcanoes of Cape Navarin, (5) Emmelen volcanoes, (6) volcanoes of the De-Longa Archipelago (Zhokhov and Vil'kitskii islands).



**Fig. 2.** Fragment of the geological map, scale 1 : 200 000. Sheets Q-58-IX and Q-58-X (*Geologicheskaya ...*, 1979). (1–3) Anyui Volcano: (1) cinder cone, (2) lava flows, (3) effusive stages (I, II, III<sub>1</sub>, III<sub>2</sub>); (4–10) sedimentary cover: (4) Upper Quaternary, alluvial sediments, (5) Hauterivian–Barremian conglomerates and sandstones, (6) Valanginian sandstones, siltstones, and shales, (7) Late Jurassic siltites, dolerites, rhyolites, sandstones, siltstones, conglomerates, tuffs, and tuff breccia, (8) Middle Jurassic sedimentary terrigenous and volcanosedimentary rocks; (9) Upper Triassic limestones and terrigenous sedimentary rocks, (10) Early Permian (P<sub>1s</sub>) dolerites, siltites, keratophyres, their tuffs, sedimentary and volcanosedimentary rocks; (11, 12) Cretaceous intrusive massifs: (11) granodiorites and granodiorite porphyry dikes, (12) diorites, quartz diorites, diorite porphyries; (1) proven, (b) inferred; (14) Mount Vulkannaya collapse cirque; (15) lakes; (16) sample numbers in Tables 1 and 2.

the study area, earliest magmatic activity is documented for the Late Jurassic (Kimmeridgian–Tithonian) and Early Cretaceous (Valanginian) (*Gelogicheskaya ...*, 1979), i.e., for the period of approximately 155–135 Ma ago. The largest part of presumed fault structures defined in the map is characterized by latitudinal or west-northwesterly strikes. The cone of Anyui Volcano is located at the fault, which crosses Mount Vulkannaya in the northeastern direction.

V.I. Sizykh (1993) assumed a single mechanism for recent volcanic activity in the Anyui group of volcanoes located within a large (130 × 160 km) ring volcanotectonic structure of the collapse caldera type. V.A. Ignat'ev (1993) also considered that volcanoes are confined to arcuate extension zones (microrifts) within a large ring fault zone. Subsequently, these researchers defined the Bolshoi Anyui ring macrostructure with Anyui Volcano on its northwestern peripheral part (Ignat'ev and Sizykh, 1997).

### STRUCTURE OF THE VOLCANO AND ERUPTION TYPE

E.K. Ustiev is the only researcher, who traced the entire lava flow from its frontal part to the volcano. Other researchers at best visited outskirts of the cinder cone. In this connection, when describing morphology of the flow, we lean upon information from (Ustiev, 1958a, 1958b, 1961, 1966) and original observations, which were carried out at a distance of up to 9 km from the crater.

Following Ustiev, most researchers (Bazarova and Vavilov, 1989; Ignat'ev and Sizykh, 1997; Grachev, 1999; Akinin et al., 2009; Okrugin and Mokhnachevskii, 2013; and others) define the following elements of the entire volcanic object in question: cinder cone (it is frequently termed as a volcano), lava flow extending from the cone in a northerly direction and partly incised into the river valley (it is sometime named as the “main flow”), and the so-called “fissure flow” observable only in the Monni River valley and extending in the sublatitudinal direction. Different authors interpret the succession of eruptions of individual lava portions not always, in our opinion, in consistency with facts. Some of them believe that Anyui Volcano represents a long-living polygenic center and that lava flow incised into the Monni River valley resulted from the Iceland-type fissure eruption. Until now, none of the available published maps contains information on sampling sites of the analyzed samples. Thus, there are several unsolved problems related to insufficient knowledge of the succession of lava flows and their eruption type. We carried out the interpretation of aerial and satellite images and propose a new reconstruction for Anyui Volcano eruptions (Fig. 2).

It is known that tectonic setting of the eruption and chemical composition of magma (silica and alkali concentrations, gas contents) represent the main factors responsible for the type and mode of eruptions. More-

over, precisely viscosity of magma determines to a significant extent the diversity of eruption products (lava, pyroclastics) and their eruption type and distribution.

Anyui Volcano is composed of the main basaltic and the subordinate basaltic andesite lavas with a relatively low share of pyroclastic material. The preserved pyroclastic products of the basaltic andesite composition characterize only the cone edifice. Correspondingly, eruption of Anyui Volcano may be characterized as a substantially effusive process. Moreover, individual lava portions differ both in morphology and chemical composition, which allows several stages to be defined in its eruption.

Eruptions resulting in the formation of edifices, such as Anyui volcano, are usually accompanied by a more or less pyroclastic activity through their entire duration (Kereszturi and Németh, 2012). However, since sections with unconsolidated rocks, which reflect the eruption record, are lacking, we are compelled to use only available lavas and remains of the cinder cone. In this connection, reconstruction of the succession in the Anyui Volcano eruption is mainly based on the succession of individual lava flows.

#### *Morphology of Lava Flows and Cinder Cone*

The eruption commenced likely as lava flow, which moved from the cone along the northwestern gully and farther downward along the Monni River valley (*Flow I*) (Fig. 2). The subsequent eruption stages are represented by lava flows, which extended from the cone in a northerly direction. *Flow II*, fissure flow, according to (Ustiev, 1961), is the longest one (56 km). Its frontal parts remained unburied under the subsequent lava portions at a distance of 36 km from the cone. *Flow III*, main flow, according to (Ustiev, 1961), advances over a distance of 20 km from the cone and includes many portions of lava, some of which are distinguishable in the relief. Inasmuch as the analytical data published in (Bazarova and Vavilov, 1989; Grachev, 1999) are scarce and lack exact indications of sampling sites, only the earliest (*Flow III*<sub>1</sub>; lavas extending along the Monni River valley) and later (*Flow III*<sub>2</sub>; lavas distributed up to 3.5–4.0 km away from the cone and hardly reaching the river valley) stages are definable in Flow III. The final, fourth (explosive–effusive) stage of Anyui Volcano eruption reflects activity of the cinder cone and two small lava bocche located near its piedmont. This stage (*IV*) was marked by the formation of cinder and lavas of the cone, which extended over a maximum distance of 1 km from the crater. It is conceivable that eruption in the main eruptive center of Anyui Volcano was accompanied by eruption of the subsidiary center located on the slope of Mount Vulkannaya 1.5 km north-northwest of the cinder cone (Fig. 2). This is the so-called Malyi Anyui Volcano.

It should be emphasized that the defined flows consist of numerous individual lava portions; i.e., they

**Table 1.** Concentrations of petrogenic oxides (wt %) and trace elements (ppm) and isotopic composition of lavas and pyroclastics from Anyui Volcano

Components	Flow I			Flow II	Flow III <sub>2</sub>						Cinder and lavas of the cone, up to 1 km from the crater				
	1	2	3	4	5	6	7	8	9	10	11	12	13	14	
	0915/1	0914/1	0916/2	06-02	U-120/15	U-125/18	0909/1	0918/1	U-122/8	0913/1	U-125/12	0910/1	U-120/5	06-01	
SiO <sub>2</sub>	49.36	50.92	51.29	51.81	51.86	52.32	52.69	52.75	53.30	53.63	53.98	54.16	55.18	55.29	
TiO <sub>2</sub>	2.09	2.18	2.18	1.57	1.49	1.88	2.02	2.04	1.51	1.74	1.62	1.65	1.78	1.60	
Al <sub>2</sub> O <sub>3</sub>	15.98	16.51	16.64	13.75	16.17	15.62	16.72	16.37	16.11	16.10	16.12	15.91	16.64	15.33	
Fe <sub>2</sub> O <sub>3</sub>	10.22	10.38	10.27	4.49	—	—	9.69	10.05	—	10.69	—	9.95	—	4.77	
FeO	—	—	—	7.56	9.13	9.27	—	—	9.38	—	7.56	—	7.26	5.05	
MnO	0.14	0.13	0.13	0.13	0.11	0.11	0.12	0.13	0.10	0.13	0.09	0.13	0.08	0.14	
MgO	6.92	3.99	3.73	7.41	6.75	6.07	3.70	3.74	5.97	4.02	6.99	5.72	5.93	5.28	
CaO	8.19	8.05	7.96	7.47	7.71	7.47	7.87	7.94	7.13	7.73	7.08	6.75	7.26	7.46	
Na <sub>2</sub> O	4.00	4.63	4.93	3.98	4.72	4.91	4.70	4.56	4.80	4.32	4.92	4.13	4.62	3.80	
K <sub>2</sub> O	2.58	2.71	2.41	1.45	1.66	1.85	2.04	2.02	1.32	1.39	1.12	1.27	0.83	1.00	
P <sub>2</sub> O <sub>5</sub>	0.51	0.48	0.45	0.37	0.41	0.48	0.43	0.39	0.37	0.25	0.51	0.32	0.42	0.27	
Cr	208.4	198	205	275.9	—	168	214.0	185	162	161	—	180.0	171	152.1	
Ni	86.9	60	55	362.7	—	—	74.42	50	—	55	—	68.3	—	103.7	
Co	42.6	26	30	39.8	—	36	41.72	23	38	22	—	40.2	39	33.8	
Sc	16.6	—	—	4.0	—	16	14.8	—	15	—	—	13.8	16	15.1	
V	167.0	140	151	130.7	—	—	145.5	125	—	115	—	129.8	—	122.8	
Li	6.4	—	—	—	—	—	8.19	—	—	—	—	8.21	—	—	
Be	1.761	—	—	1.27	—	—	1.48	—	—	—	—	1.25	—	1.32	
Cs	0.266	—	—	0.20	—	—	0.179	—	—	—	—	0.145	—	0.200	
Rb	20.241	23	20	14.67	—	15	14.9	19	11	10	—	8.8	9	15.8	
Ba	322.8	363	340	194.5	—	—	239.15	242	—	190	—	144.8	—	160.27	
Sr	650.0	653	636	487.3	—	528	556.25	561	465	471	—	395.3	464	386.04	
U	1.176	—	—	0.645	—	0.8	0.881	—	—	—	—	0.626	1.1	0.564	
Th	3.446	—	—	1.835	—	2.4	2.477	—	2.2	—	—	1.657	2.5	1.791	
Pb	3.369	2	5	0.573	—	—	3.690	2	—	8	—	2.815	—	1.408	

Table 1. (Contd.)

Components	Flow I		Flow II	Flow III <sub>2</sub>					Cinder and lavas of the cone, up to 1 km from the crater					
	1	2	3	4	5	6	7	8	9	10	11	12	13	14
	0915/1	0914/1	0916/2	06-02	U-120/15	U-125/18	0909/1	0918/1	U-122/8	0913/1	U-125/12	0910/1	U-120/5	06-01
Ta	3.055	—	—	1.522	—	1.8	2.260	—	1.5	—	—	1.552	1.4	1.015
Nb	44.5	35	29	25.6	—	—	30.076	26	—	17	—	20.7	—	19.1
Hf	4.77	—	—	2.58	—	3.3	3.850	—	2.5	—	—	3.086	2.6	2.59
Zr	208.3	180	183	132.9	—	—	168.82	160	—	133	—	128.47	—	114.1
Y	15.9	20	20	15.2	—	—	13.6	22	—	15	—	11.98	—	14.0
La	25.61	—	—	14.76	—	16	18.59	—	13	—	—	12.60	12	10.55
Ce	49.82	—	—	28.25	—	33	37.71	—	27	—	—	26.14	21	21.17
Pr	6.38	—	—	3.59	—	—	4.76	—	—	—	—	3.47	—	2.85
Nd	27.13	—	—	15.89	—	23.03	20.40	—	19.6	—	—	16.64	18.38	13.62
Sm	5.92	—	—	4.21	—	6.09	5.28	—	5.58	—	—	4.54	5.38	3.95
Eu	2.01	—	—	1.49	—	1.9	1.84	—	1.8	—	—	1.69	1.9	1.43
Gd	5.87	—	—	4.02	—	—	5.40	—	—	—	—	4.71	—	3.78
Tb	0.84	—	—	0.58	—	0.81	0.77	—	0.81	—	—	0.66	0.82	0.56
Dy	4.22	—	—	3.218	—	—	3.83	—	—	—	—	3.37	—	2.971
Ho	0.79	—	—	0.568	—	—	0.70	—	—	—	—	0.597	—	0.536
Er	1.97	—	—	1.34	—	—	1.690	—	—	—	—	1.469	—	1.337
Tm	0.24	—	—	0.178	—	—	0.195	—	—	—	—	0.182	—	0.181
Yb	1.469	—	—	1.016	—	1.3	1.272	—	0.92	—	—	1.094	1.3	1.041
Lu	0.210	—	—	0.137	—	0.2	0.175	—	0.1	—	—	0.153	0.18	0.136
<sup>87</sup> Sr/ <sup>86</sup> Sr	0.703589	—	—	0.703961	—	0.703796	—	—	0.704346	—	—	—	0.704485	0.705099
<sup>143</sup> Nd/ <sup>144</sup> Nd	0.512966	—	—	0.512891	—	0.512902	—	—	0.512860	—	—	—	0.512827	0.512704
εNd	6.4	—	—	4.9	—	5.1	—	—	4.3	—	—	—	3.7	1.3

(1–3, 7, 8, 10, 12) collection of M.M. Pevzner; (4) collection of M.I. Tuchkova (Fedorov and Koloskov, 2009); (5–6, 9, 11, 13) collection of A.A. Surin (Grachev, 1999); (14) collection of A.V. Lander (Fedorov and Koloskov, 2009). Petrogenic elements were analyzed at Institute of Geology of Ore Deposits, Petrography, Mineralogy, and Geochemistry of the Russian Academy of Sciences (IGEM RAN) (1–3, 7, 8, 10, 12); Geological Institute of the Russian Academy of Sciences (GIN RAN) (4, 14); and Industrial Geological Trust Sevmorzapgeologiya (St. Petersburg) (5, 6, 9, 11, 13). Trace elements were investigated by the RFA method at IGEM RAN (2, 3, 8, 10) and Sevmorzapgeologiya, St. Petersburg (5, 6, 9, 11, 13) the ICP-MS method at the Institute of Mineralogy, Geochemistry, and Crystallochemistry of Trace Elements of the Russian Academy of Sciences (IMGRE RAN) (4, 14); and Analytical Certification-Testing Center of the Institute of Microelectronics Technology Problems and High Purity Materials of the Russian Academy of Sciences (1, 7, 12); and the NAA method at Sevmorzapgeologiya, St. Petersburg (5, 6, 9, 11, 13). Isotopic investigations were performed at the Institute of Precambrian Geology of the Russian Academy of Sciences (1, 4; analyst E.S. Bogomolov; 6, 9, 11, 13; analyst B.V. Belyatskii) (Grachev, 1999) and the Vernadsky Institute of Geochemistry and Analytical Chemistry of the Russian Academy of Sciences (GEOKhl RAN) (14; analyst S.F. Karpenko). Composition of petrogenic elements is recalculated for the “water-free” residual; (–) not analyzed.

**Table 2.** Concentrations of petrogenic elements (wt %) in lavas and pyroclastics from Anyui Volcano

Component	Flow I		Flow II	Flow III <sub>1</sub>	Flow III <sub>2</sub>			Cinder and lavas of cone, up to 1 km from the crater				Parasitic cone
	1	2	3	4	5	6	7	8	9	10	11	12
	28	51	4	53	6	5	10	40	41	3	15	1248
SiO <sub>2</sub>	49.41	50.50	52.34	53.28	52.06	52.15	52.36	54.07	54.31	54.01	54.95	53.40
TiO <sub>2</sub>	2.23	2.02	1.67	1.59	1.87	1.84	1.90	1.50	1.61	1.62	1.62	1.46
Al <sub>2</sub> O <sub>3</sub>	15.44	15.27	15.58	15.66	15.86	16.02	16.02	15.69	15.23	15.92	15.87	16.19
Fe <sub>2</sub> O <sub>3</sub>	1.44	0.85	1.62	1.90	—	—	—	5.31	1.73	—	—	7.61
FeO	8.73	9.99	8.06	7.32	9.79	9.52	9.34	4.66	8.10	9.22	8.95	4.07
MnO	0.16	0.18	0.12	0.14	0.15	0.15	0.15	0.13	0.14	0.15	0.15	0.15
MgO	7.20	7.13	6.49	6.62	6.28	6.58	6.16	5.96	5.92	6.20	5.88	6.03
CaO	8.37	7.49	8.04	7.26	7.71	7.63	7.77	7.26	7.52	7.35	7.36	6.21
Na <sub>2</sub> O	3.71	3.69	3.61	3.69	3.95	3.81	3.92	3.53	3.73	3.77	3.54	3.36
K <sub>2</sub> O	2.55	2.39	1.87	2.08	1.88	1.84	1.93	1.47	1.40	1.35	1.29	1.25
P <sub>2</sub> O <sub>5</sub>	0.77	0.49	0.59	0.45	0.45	0.46	0.45	0.41	0.31	0.41	0.38	0.27

Samples: (1–4, 8, 9), after (Ustiev, 1961); (5–7, 10, 11); after (Bazarova and Vavilov, 1989); (12) collection of A.T. Khitrinov (Dovgal and Chasovitin, 1965). Composition of petrogenic elements is recalculated for the “water-free” residual; (–) not analyzed.

reflect large eruption stages. Let us consider these stages in more detail.

**Flow I.** The earliest lava portions are documented and sampled (Table 1, no. 3; Table 2, no. 1) in the creek valley oriented in the northwestern direction from the cinder cone (Fig. 3). Downslope, this flow reaches the Monni River valley and spreads further in the western direction (Table 1, nos. 1, 2). The flow in question is buried under later lavas. It is best observable at the exit from the creek valley and near the left slope of the river valley 5 km away from the cone. The chemical composition of earlier lava portions (low contents of silica and high contents of K) also implies the presence of Flow I at least 18–20 km away from the cinder cone (Table 2, no. 2). Exposed areas of Flow I are largely represented by pahoehoe lavas with peculiar features: wavy surface frequently deformed into folds, presence of abundant tunnels and tubes (locally with the collapsed top), fragments of corded pahoehoe, and shiny glassy crust (Fig. 4). The ends of lava tunnels are frequently represented by the “road”-type surface consisting of smooth lavas. Locally, the relatively smooth surface of such lavas demonstrates five- and six-faceted jointing. The flow is heterogeneous: it is composed of many alternating thin (<1 m) lava portions. In our opinion, the significant scatter of data obtained during the sampling of lavas from Flow I indicates multiphase eruptions. This aspect is more thoroughly considered below. The length of Flow I along the creek valley from the cone to the Monni River valley is approximately 4.5 km and the difference between these points could be at least 500 m. Thus, the average altitude gradient along the creek valley exceeded

100 m/km, which allowed lavas to reach rapidly the river valley. It may be assumed that lavas of early portions extended along the valley at least over 15 km. In this area, the altitude gradient was substantially lower (8 or 9 m/km). Nevertheless, this is a relatively steep incline sufficient for lavas to spread and fill the valley.

**Flow II.** This is the longest lava flow (56 km) filling the Monni River valley (Fig. 2). Its lavas were sampled in the frontal part of the flow (Table 1, no. 4) and 13 km upstream the valley (Table 2, no. 3). The head part of the flow is buried under younger lavas, although the most distant areas of the lava field (36 km away from the cone) are preserved in their initial state. The structures and morphology of the flow are described in (Ustiev, 1958a, 1958b, 1961, 1966). According to these descriptions, Flow II is formed by lavas of different types: aa, pahoehoe, and block lavas. Areas of block and aa lavas were likely formed owing to the break in eruption and relatively rapid cooling of individual lava portions, which met an insurmountable obstacle. For example, (Ustiev (1961) noted lava blocks up to 1 or 2 m across near the flow front.

The length of the lava flow along the Monni River valley from Lake Kukol to its front is approximately 52 km. The height difference between these points amounts to 330 m. Thus, the average altitude gradient along the valley exceeded 6 m/km, which allowed liquid basaltic lavas to extend almost freely over large distances.

Lavas of Flow II incised into the Monni River valley are characterized by the basaltic composition (Tables 1, 2), which implies low viscosity. The lava section represents a succession of many thin liquid

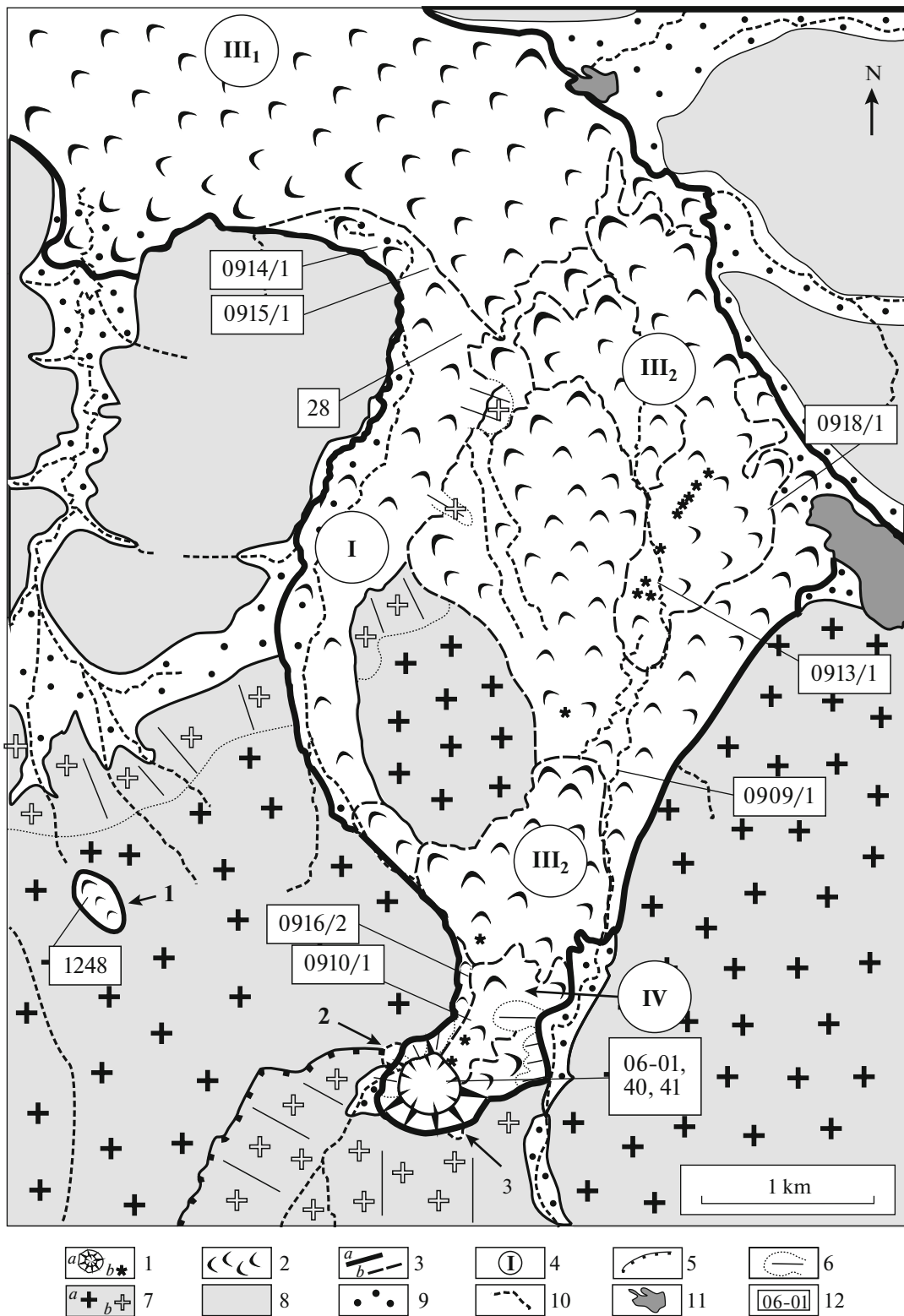


**Fig. 3.** Schematic distribution of lavas near the cinder cone of Anyui Volcano. (1) Eruptive centers: (a) cinder cone, (b) bocche; (2) lavas; (3) boundaries: (a) lava field, (b) individual lava portions; (4) eruption stages; (5) fragment of the northwestern edge of the Mount Vulkannaya collapse cirque (Fig. 2); (6) rockslide–talus forms; (7) Cretaceous granitoids of Mount Vulkannaya: (a) in situ, (b) rockslide–talus sediments; (8) Upper Triassic sedimentary rocks; (9) proluvial and volcanogenic–proluvial deposits; (10) creeks; (11) lakes; (12) numbers of samples, which are provided with accurate GPS or topographic information (Tables 1 and 2). Numerals on the figure: (1) position of Malyi Anyui Volcano, (2) “ballistic ejects” shown in Fig. 9, (3) fragment of the cone shown in Fig. 8.





**Fig. 4.** Lavas of the initial stage of Anyui Volcano eruption. Flow I, fragment of wavy lavas at the mouth of the water gap. Photo by D.O. Gertsev.

flows (thickness of individual lava portions never exceeds 1 m), which spread as separate flows along local depressions. The earliest lava portions filled the lowest areas and formed a new profile of the valley. Next portions of lava flowed around these newly formed obstacles and gradually filled the entire Monni River valley. Simultaneously, new lava portions continued to enter and build up the valley bottom. As a result, individual lava “creeks” spreading downward the valley and meandering in search of depressions started to flow into the feathering water gaps. New portions of hot lava contacted the older portions that started to cool down, but were still plastic, resulting in the formation of numerous folds and wrinkles oriented in different directions and the development of the “astrakhan”-type appearance of the flow surface (Fig. 5a). Similar structures are also observable on other liquid lava flows of the basaltic composition (Fig. 5b).

Ustiev (1961) attributed the formation of this lava flow to a fissure system and even defined it as the “fissure” flow. He noted the presence of granite dikes confined to sublatitudinal tectonic fractures in the volcano area. Proceeding from this observation, the author assumed the presence of similar “longitudinal fractures, which appeared (or were renewed) in response to recent tectonic movements” and were also

responsible for “fissure eruptions at the valley bottom” (Ustiev, 1961, p. 8).

At the same time, aerial images demonstrate clearly that the structures, which could result from fissure eruption (linear structures with associated cinder and cinder-lava cones), are missing along the entire Flow II. Figure 5a illustrates a fragment of Flow II with the largest, in the opinion of Ustiev (1961), fissures. Indeed, longitudinal structures are observable along the northern slope of the field, but they represent rather wrinkles of lava folds in Flow I formed during the movement of later Flows II and III<sub>1</sub>; i.e., they are a sort of “squeezing” or “bulldozer” facies. If this assumption is correct, it becomes clear that the time gap between eruptions of lavas of Flows I and II was very short, since lavas of Flow I still preserved plasticity. The presence of lavas of Flow I in the area under discussion is confirmed by the chemical analysis of the sample (Table 2, no. 2) taken near the front of Flow III<sub>1</sub> (Fig. 2).

Figure 5b shows for comparison the plan view of the fissure responsible for the eruption in the Grimsvotn caldera (Iceland) in 1783–1785. This is the famous Laki fissure. Eruption associated with this fissure was thoroughly investigated in (Thordarson and Self, 1993) and is considered a classical example of fissure eruptions. The Laki fissure (25 km long) is represented by a chain

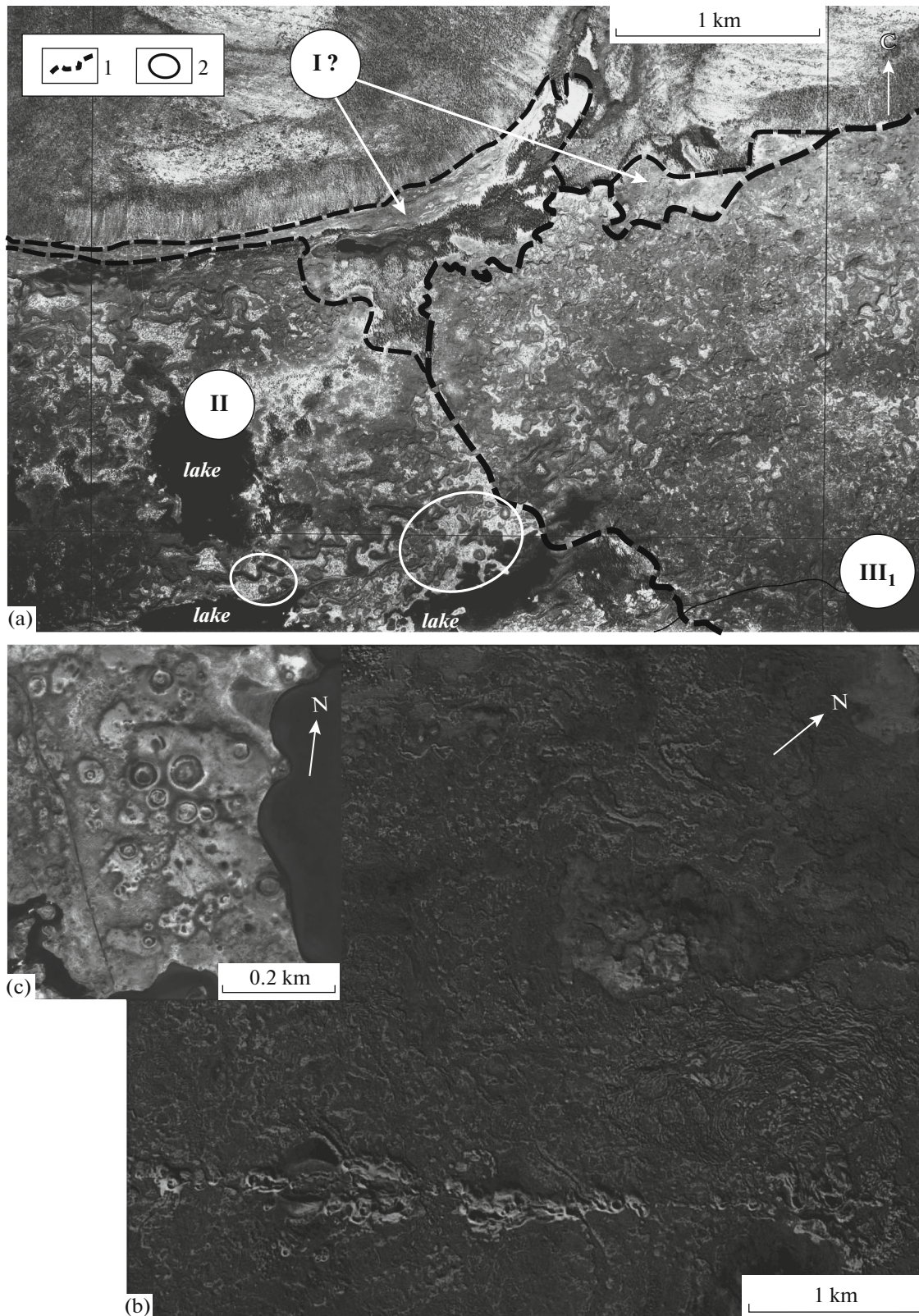


**Fig. 5.** Fragments of basic lava flows.  
 (a) Anyui Volcano, 7 km west of Lake Gornoe. Aerial photo: (1) boundaries of Flows I, II, and III<sub>1</sub>; (2) groups of pseudocraters;  
 (b) eruption in 1783 from the Laki fissure (Grimsvötn caldera, Iceland); (c) eruption of Krafla Volcano 2100 yr ago, pseudocraters  
 in Lake Mývatn (Iceland).

of about 100 cinder and cinder-lava cones towering above the lava flow surface for 80–90 m rather than by an open crack. Nothing resembling such a volcanic structure is observed in any lava flow of Anyui Volcano. The presence of additional eruptive centers is not needed for explaining the existence of the lava flow 56 km long. Extended (dozens of kilometers long) liquid basaltic lava flows, which erupted from bocche and adjacent small fissures, are relatively frequent in Siberia, e.g., the 80-km-long Zhom-Bolok “lava river” in the Sayany Mountains (Yarmolyuk et al., 2003; Ivanov et al., 2011). Possibility of the formation of such “lava rivers” is determined by the outflow of liquid lavas in valleys with a significant altitude gradient. Aeromagnetic investigations in the Anyui Volcano area carried out in 1959 and 1964 yielded no data in favor of the existence of faults and fissures, which could give birth to the lava flow in the Monni River valley (Ignat’ev and Sizykh, 2001).

Then, why Ustiev emphasized the presence of fissures? This is most likely explained by the fact that he never studied young volcanism prior to his first study. Geologist visiting for the first time a well-preserved lava flow discovers for himself the quite unimaginable world of a giant rocky labyrinth of capricious accumulations of blocks and obelisks, rampant lava waves and bubbles, as well as narrow deep gorges and lava tunnels. Undoubtedly, such a rocky splendor can mislead an inexperienced investigator. Nevertheless, expressive description of the flow morphostructures by Ustiev is of great significance, since it provides an idea of the outlook of individual elements on the flow surface.

For example, Flow II demonstrates wide distribution of the so-called “lava lakes” (Ustiev, 1961). One of them is represented by a cylindrical hole up to 150 m across and approximately 15 m deep. The hole is surrounded by a wide concentric swell up to 5 m high. Ustiev describes that “...the hole bottom is very uneven and mostly resembles a pot with intensely boiling tar; capricious hummocks alternate with similar deeps and corded structures are oriented in different directions. The almost even surface of basalts is perforated by densely spaced round holes. Therefore, it amazingly resembles bee honeycombs. The holes are 8–10 mm in diameter. In areas, where basalts are crossed by open fissures, the holes are tubular and extend deep into the flow, probably, up to its base. ...The appearance of such holes, which usually perforate the lower part of the flow, is attributed to gases. When hot lavas fill the wet valley bottom, a huge amount of water vapor is produced. In the absence of other exit, it can penetrate the liquid lava flow and escape in the form of strong jets” (Ustiev, 1966, pp. 151, 152). These remarkable observations allow the morphostructures to be interpreted as phreatic pseudocraters (Thorarinnsson, 1953) related to the contact of hot lava with the groundwater-saturated surface or frost ground. The most famous group of pseudocraters related to phreatic explosions is located on Lake Mývatn in Iceland

(Fig. 5c). They were formed during the eruption of Krafla Volcano 2100 yr ago (Thordarson and Hoskuldsson, 2008). The average diameter and depth of pseudocraters in Anyui Volcano are approximately 100 and 10 m, respectively. They frequently make up groups and occur near lakes (Fig. 5a). The presence of many phreatic pseudocraters is an important morphological feature of Flow II.

**Flow III**, which was considered by Ustiev (1961) as the “main” flow, extends over 20 km from the cone. It is composed of many lava portions including those observable in the relief. The scarce data allow only the earlier (Flow III<sub>1</sub> represented by lavas extending from the cone in a northerly direction and filling the Monni River valley) and later (Flow III<sub>2</sub> composed of lavas distributed also from the cone in a northerly direction over a maximum distance of 3.5–4.0 km and hardly reaching the river valley) stages to be defined in Flow III.

Satellite and aerial images (Fig. 5a) demonstrate clearly that Flow III<sub>1</sub> incised into the Monni River valley is virtually devoid of pseudocraters. This implies that lavas of Flow II moved through areas saturated with groundwater, while no such contact existed between lavas of Flow III<sub>1</sub> and the underlying surface. It is also seen that Flow III<sub>1</sub> is heterogenic and consists of several large successive lava portions. Figure 5a shows the front of this flow. According to (Ustiev, 1961), it is 15–20 m high. Similar, although probably thinner, fronts are definable at the latitude of lakes Gornoe and Zaprudnoe (Fig. 6). Frontal portions of individual flows are less expressed upstream the river valley. The creek flowing into Lake Zaprudnoe demonstrates clearly why lava flows changed their directions and deviated to the feathering water gaps in the valley. New portions of lavas leaning against the older cooling lavas were forced to deviate and enter the water gap mouth.

Flow III<sub>1</sub> consists of lavas belonging to different types: aa, pahoehoe, and block varieties (Ustiev, 1961). In aerial images, it seems slightly more viscous than the underlying Flow II.

Lavas of Flow III<sub>1</sub> were likely sampled by Ustiev near its front (Table 2, no. 4). We doubt that the sample was taken precisely from the portion under consideration: “lava was sampled from the bottom of a deep cleft near the front of the main flow” (Ustiev, 1961, p. 77); i.e., one cannot rule out that the sampled rock could belong to earlier eruptions (Flow II). Available data on the chemical composition (Tables 1, 2) obtained during different years in different laboratories by different methods cannot serve as basis for the detailed geochemical correlations. The head part of the flow is buried under later lavas of Flow III<sub>2</sub>. The length of Flow III<sub>1</sub> from Lake Kukol to its front is approximately 16 km and the height difference exceeds 100 m; i.e., the altitude gradient is almost 7 m/km.

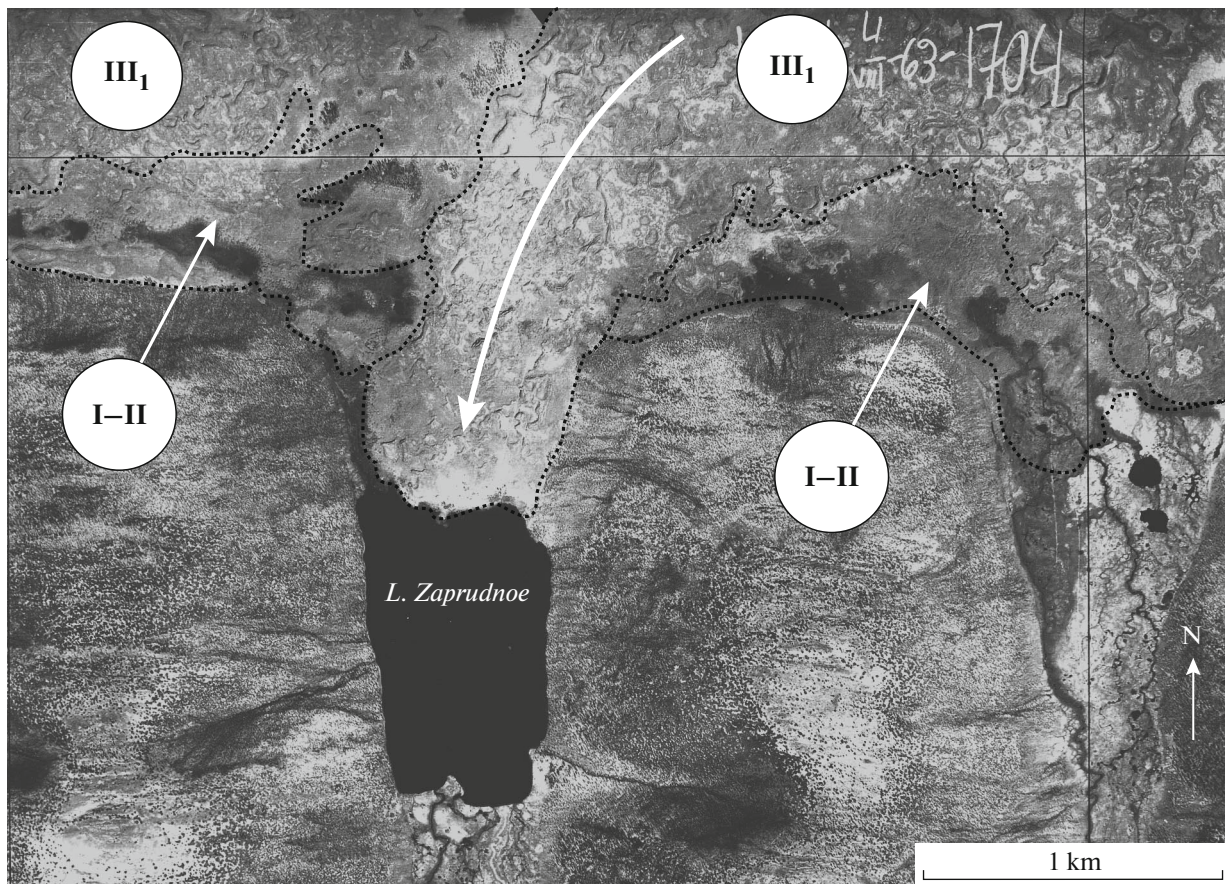


**Fig. 6.** Fragment of lava flows of Anyui Volcano at the latitude of Lake Zaprudnoe, aerial photo. Arrow indicates the direction of movement of individual lava portion of Flow III<sub>1</sub>.

Contacts of Flows I, II, and III<sub>1</sub> are readily recognizable in the relief (Fig. 5a). Therefore, the stratigraphic succession of these large effusive stages is undoubted. Nevertheless, the intricate structure of the flows requires verification of their defined contours in the field.

Flow III<sub>2</sub> unites lavas extending from the cone over a maximum distance of 3.5–4 km in a northerly direction up to the valley entrance. The northern piedmont of the cone is complicated by a buried bocca, which served as an eruption center for lavas of Flow III<sub>2</sub> (it is highly probable that this area was a subsidiary rather than main lava eruption center of Flow III<sub>1</sub>). The axial part of the flow exhibits a small fissure marked by a dozen small lava bocche (Fig. 3). The flow is largely represented by fragmented aa lavas with a peculiar uneven surface composed of densely spaced size-variable (up to 1.0–1.5 m) blocks. Their surface is frequently rough due to friction between the moving hot blocks. Thickness of such crust never exceeds a few centimeters. Small “grated” fragments play the role of cement in large blocks. The smallest blocks are sometimes strongly polished and devoid of acute facets. Therefore, they cannot be attributed to the later

destruction of rocks. Virtually similar blocks are observable in the lava section at contacts of individual lava portions; i.e., the transformation of these fragments was determined by peculiarities in the lava movement and cooling. The flow in question also exhibits areas of smooth lavas, in addition to aa lavas. These areas yielded perfectly preserved glazed lava “icicles.” Small areas occupied by large blocks are located near the cinder cone.

Lava is highly porous and mostly oxidized. In the canyon of a dry river, which crosses the flow, it is seen that the flow consists of numerous thin (0.1–0.8 m) lava portions separated by bright ochreous and overheated contact zones (Fig. 7). The canyon hosts well-rounded blocks, which resulted undoubtedly from activity of the intermittent water flow.

Our sampling revealed that lavas become successively more acid closer to the cone. This trend was used for the positioning of samples (Bazarova and Vavilov, 1989; Grachev, 1999) only provided with the reference “lavas of the main flow of Anyui Volcano.” Flow III<sub>2</sub> is composed of basaltic andesites (Table 1, nos. 5–10; Table 2, nos. 5–7). It is up to 4 km long and height difference between the head and front is



**Fig. 7.** Section of lava Flow III<sub>2</sub> formed by small successive lava portions with distinct contact zones between individual flows. Overheated contact zones are seen between some flows. Apparent thickness 3 m. Photo by D.O. Gertsev.

approximately 4000 m (gradient 100 m/km). It seems that increased viscosity of lavas was responsible for their stop at the entrance into the valley, as opposed to preceding portions characterized mostly by a more basic composition and, consequently, lower viscosity. Areas of pahoehoe lavas within contours of Flow III<sub>2</sub> could be related to very high velocity of basaltic andesite lavas due to the strong incline of the surface. At the same time, one cannot rule out the possibility that they represent areas of earlier phases (unburied under Flow III<sub>2</sub>), when pahoehoe lavas were more widespread.

Some lava portions cannot confidently be attributed to the defined phases: the succession of their eruptions may only be established by field observations with an obligatory study of their chemical compositions. For example, phase III was characterized at its end by the eruption of lavas that flowed along the western gully to overlie partly the surface of Flow I (Fig. 3). These lavas were not sampled and their place in the general history of eruption remains unknown.

**Cinders and lavas of the cone**, which accumulated during the terminal stage of the eruption (stage IV), extend over 1 km from the crater (Fig. 3). This explosive-effusive stage is related to the activity of both cin-

der cone proper and a pair of small lava bocche located near its northeastern piedmont.

Rocks of stage IV are represented by basaltic andesites (Table 1, nos. 11–14; Table 2, nos. 8–11). The most “acid” sample (Table 1, no. 14) is a cinder-lava bomb from the cone. The only sample of tephra (Table 1, no. 12) was taken at the contact between lavas of later portions 50 m away from the cone piedmont. The rock represents juvenile gravel-sized cinder and black light porous, unoxidized lapilli with oily luster. This tephra is likely related to terminal stages of cone activity, while pyroclastics of the paroxysmal phase is partly buried under lava flows and partly washed out by meltwater. Sample nos. 8 and 9 (Table 2), which were attributed by Ustiev to the “fissure” flow (Flow II) (i.e., the initial, in his opinion, phase of effusive activity), reflect this terminal eruption stage as well. At the same time, according to (Ustiev, 1961), sample no. 8 represented by “... finely porous lava of the volcanic cone” (p. 109) is “... oxidized red-colored lava” (p. 95) and sample no. 9 is “... finely porous lava of the volcanic cone” (p. 109) ... “from the volcano vent” (p. 65). We attributed sample nos. 11 and 13 (Table 1), as well as sample nos. 10 and 11 (Table 2), which lack indications of sampling places and coordinates, to the terminal stage of eruption based on the similarity of their chemical composition with that of

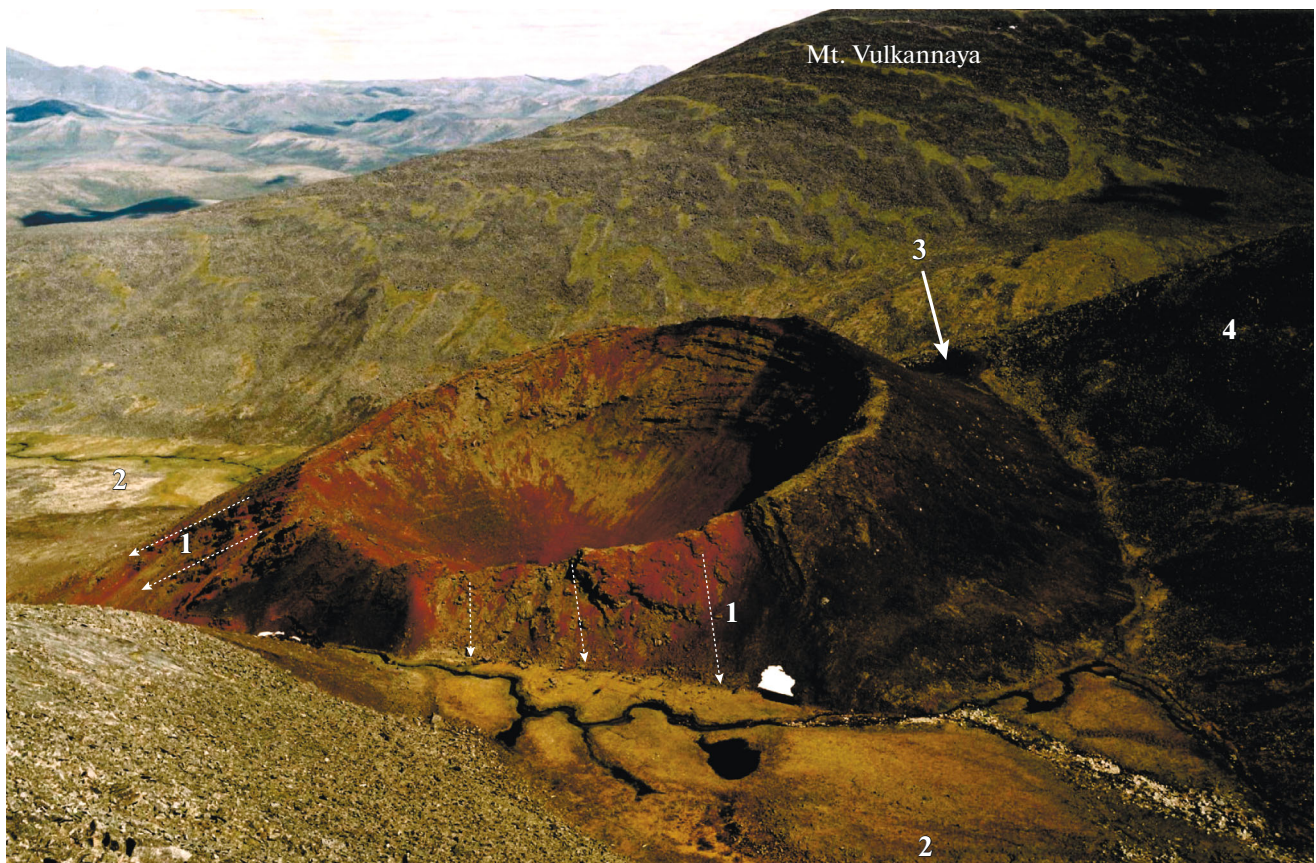


**Fig. 8.** Cinder cone of Anyui Volcano. View from the west. In the background, slopes of Mount Vulkannaya and far summits of the South Anyui Range. Photo by S.M. Katkov.

(1) Traces of the collapse of the cone edifice; (2) volcanogenic–proluvial depressions; (3) fragment of the initial cinder cone; (4) rockslide–talus deposits. For location of these objects in the map, see Fig. 3.

the sample taken from cone cinder and lavas at a distance up to 1 km away from the crater.

The cone is now composed of mostly brown-red welded compact agglutinates of the near-vent facies. Moreover, it is virtually devoid of the unconsolidated (substantially black) cinder cover, which is characteristic of young (Holocene) cones (Fig. 8). Cinders (tephra) are absent on the cone proper and neighboring rises and in creeks. The lower two-third of the cone edifice is largely composed of pyroclastic material, which implies normal explosive activity. The upper one-third of the cone (the highest southeastern wall) consists of alternating pyroclastics and thin intercalations of lava-type material. It seems that the terminal phase of cone activity was characterized by weakened explosive intensity and incandescent fall of ballistic ejecta (cinder-lava bombs) near the crater. Due to high temperature, they could weld and even form lava-type flows, which shielded the cinder cone by a compact crust and guaranteed its relatively good preservation. Inasmuch as such rocks result from relatively weak explosions, unidirectional ejecta can hardly be expected. Most likely, the cone was regularly covered

by bombs and lava-type crust. Nevertheless, the crust is now absent on the north-northwestern slope of the cinder cone, which implies a significant destruction of this segment. The crater edge in this area is located at the altitude of approximately 1000 m, while maximal height of the cone amounts to 1054 m.

The bedrock slope of Mount Vulkannaya north-west of the cone clearly exhibits a spot of welded cinder-lava rocks (Fig. 9). Moreover, altitude of this spot and the upper (south-southeastern) edge of the crater is virtually (approximately 1050 m). Ustiev (1961) interpreted these rocks as “ballistic ejecta” related to activity of the inclined lava fountain. In our opinion, they represent a fragment of the lava-type crust on western slopes of the primary cone that initially leaned against the slope. Comparison of compositions of the material from this “spot” and lava-type rocks of the cone will make it possible to solve this problem. The most intense destruction of the northwestern part of the cone and the western incline of the crater are more logically explainable by the existence of the strongest meltwater flow, which already formed the canyon-shaped channel downstream of the valley (Fig. 3), in



**Fig. 9.** Preserved traces of cinder cone leaning against the bedrock slope. Arrow indicates “ballistic ejecta” preserved northwest of the cone. Photo by D.O. Gertsev. For location of the object in the map (Fig. 3).

the past (and exists now precisely in this area west of the preserved cone) rather than by the northwestern incline of the vent (Ignat’ev and Sizykh, 1997). Figure 8 clearly illustrates detachment planes of local rockslides from the western and northwestern slopes of the cone. It is noteworthy that proper rockslide deposits are completely missing from this area. They were probably removed by powerful mudflows rather than an older small creek. The mudflows could hardly be formed in the Holocene because of precipitation deficiency in this area.

Figures 3 and 8 clearly show that the southwestern piedmont of the cone is overlain by younger rockslide–talus deposits, i.e., the true diameter of the cone is unobservable in this segment. Thus, it may confidently be assumed that the primary cone could be notably larger than the present-day preserved edifice.

The following minimum parameters are assumed for the primary cone:  $H \geq 150$  m,  $D$  500–600 m,  $d \leq 300$  m, and  $h$  80–100 m, where  $H$  is the cone height,  $D$  is the base diameter,  $d$  is the crater diameter, and  $h$  is the crater depth. With such parameters, the volume of Anyui Volcano should be approximately  $0.01 \text{ km}^3$ . Parameters of Anyui Volcano are close to their values in the cone ( $0.012 \text{ km}^3$ ) formed by the southern breakthrough of the Great Fissure Tolbachik Eruption in

1975–1976 (*Bol’shoe ...*, 1984). With account for ballistic ejecta, cinder outliers, and tephra, the total volume of pyroclastic material is estimated at  $0.031\text{--}0.048 \text{ km}^3$  (*Bol’shoe ...*, 1984). It is logical to assume that the integral effect of the explosive phase of Anyui Volcano could be similar (at least  $0.03 \text{ km}^3$ ). Tephra associated with this eruption should be distributed over dozens of kilometers away from the eruptive center, while the surrounding areas should be covered by a continuous cinder cover.

**Malyi Anyui Volcano.** According to (Dovgal and Chasovitin, 1965), geologist A.T. Khitrinov (1962) discovered on the western slope of Mount Vulkannaya blocks of basaltic andesite from the “parasitic cone,” which was subsequently named as Malyi Anyui Volcano (Figs. 2, 3). According to Ignat’ev (1990), this volcanic edifice is significantly destroyed and represented now by the accumulation of angular and fritted blocks of gray vesicular basaltic andesite and cinder cement of the similar composition. Accumulation of blocks is traceable as a “tongue” 30–150 m wide and up to 370 m long extending in the northwestern direction. The eruption center is virtually unpreserved. Unfortunately, we failed to visit this area and, thus, cannot add anything to the available information. Analytical data on the chemical composition of lavas are presented in

Table 2 (no. 12). It is quite conceivable that this subsidiary breakthrough appeared simultaneously with the eruption of Anyui Volcano. Proceeding exclusively from the similarity of chemical compositions of rocks, it may be assumed that Malyi Anyui Volcano could be formed at the terminal stages of the eruption under consideration (III<sub>2</sub>–IV). The fact that the eruptive center is destroyed and represented only by the accumulation of blocks can indicate its pre-Holocene age

#### *Duration of Eruption*

Thus, the history of the Anyui Volcano eruption is in general reconstructed with the consideration of successive eruptions of different lava flows and some peculiar features in the formation of the cinder cone. It is evident that Anyui Volcano represents a monogenic center with the largest share of its lava eruption from bocche located in the immediate vicinity to the cinder cone. According to (Ustiev 1961), the integral area occupied by the lava field is 107.5 km<sup>2</sup> and the total volume of igneous rocks amounts to approximately 3.5 km<sup>3</sup>. Our calculations of flow areas using a measuring grid appeared to be very close to the above-mentioned data. Unfortunately, no measurements of the lava flow thickness were conducted during field investigations. Therefore, accurate estimate of the integral volume of lavas is impossible. How long could last this eruption?

During the historical time, similar eruptions lasted usually 9–18 months. For example, the Laki fissure was active since June 1783 to February 1784 (Hamilton et al., 2010; Thordarson and Self, 1993); and fissure eruptions on Tolbachik Volcano, from July 1975 to December 1976 (*Bol'shoe ...*, 1984) and from November 2012 to September 2013 (Gordeev et al., 2013). Eruptions of some volcanoes, such as Krafla in Iceland in 1724–1729 and 1975–1984 (Thordarson and Hoskuldsson, 2008; Thordarson and Larsen, 2007) and Timanfaya on Canary Islands in 1730–1736 (Carracedo et al., 1992) represented a series of rare short activation episodes lasting 5–10 yr in total.

The aforesaid provides grounds for an assumption that eruption of Anyui Volcano lasted several months or several years. Was this eruption continuous as, for example, on Tolbachik Volcano or discrete as on Krafla Volcano cannot reliably be established. Nevertheless, some peculiar features of the composition of Anyui Volcano lavas make the second scenario more preferable, i.e., relatively prolonged (a few years) and, probably, discrete eruption.

### COMPOSITION OF IGNEOUS ROCKS

Figure 2 shows that the lava field and cinder cone of Anyui Volcano, as well as the subsidiary eruptive center, were sampled insufficiently for the detailed characteristic of rock composition and the reconstruc-

tion of magmatic activity. Moreover, accurate GPS and topographic data are available only for some samples presented in Tables 1 and 2 (Fig. 3). For example, the chemical analyses in (Bazarova and Vavilov, 1989; Grachev, 1999) characterize lavas of the so-called main flow of Anyui Volcano. According to (Ustiev, 1961), the “main flow” is approximately 20 km long. On the basis of some above-mentioned features, it may be divided at least into stages. However, because of the absence of accurate geographic data on sampling places in (Bazarova and Vavilov, 1989; Grachev, 1999), we were forced to unite these flows into a single stage (III) subdivided into two successive phases (III<sub>1</sub> and III<sub>2</sub>). Our sampling (Fig. 3) revealed that lavas become successively more acid toward the cone. Based on this trend, we attributed conditionally samples mentioned in (Bazarova and Vavilov, 1989; Grachev, 1999) to the late phase of stage III (III<sub>2</sub>) and terminal stage IV (cinders and lavas of the cone). The chemical analytical data from (Okrugin and Mokhnachevskii, 2013) are ignored in this work, since they lack geographic indications and laboratory information. At the same time, the analytical results in (Okrugin and Mokhnachevskii, 2013) agree well with the data presented in Tables 1 and 2 and do not basically change the general characteristic of rocks.

The analytical data presented in Tables 1 and 2 were obtained in different years in different laboratories and by different methods. Nevertheless, even such heterogeneous data are sufficient for the general characteristic of some chemical properties of rocks and magma generation.

Cinders and lavas from Anyui Volcano are represented by subalkali basaltic andesites and basalts. Phenocrysts are composed of andesine-labradorite, pigeonite augite (Wo<sub>38–44</sub>En<sub>33–50</sub>Fs<sub>11–23</sub>) and olivine (from Fo<sub>82–85</sub> to Fo<sub>78–60</sub>) (Akinin et al., 2008; Bazarova and Vavilov, 1989). All minerals of phenocrysts contain primary inclusions with the phase composition represented by glass, liquid CO<sub>2</sub> (T<sub>hom</sub> approximately +18°C, specific volume 1.25 cm<sup>3</sup>/g) and solid-phase inclusions (Bazarova and Vavilov, 1989). Ore minerals occur as small black cubic crystals of magnetite and skeletal structures of hematite. The groundmass texture and quantitative phenocryst composition correlate distinctly with the position of rocks in the flow. Maximum (up to 77–78%) and minimum (23–13%) contents of volcanic glass are characteristic of the vesicular and compact lavas varieties, respectively (Akinin et al., 2008; Ustiev, 1961).

Petrochemical properties of effusive rocks of Anyui Volcano are presented in (Tables 1, 2; Figs. 10, 11). Data points of their compositions are localized near the line separating the subalkaline and alkaline series (Irvine and Baragar, 1971) (Fig. 10a) as several isolated areas: lavas of stages I–III and basaltic andesites of the cinder cone attributed to stage IV. According to the petrochemical classification, lavas from flows of stages I–III



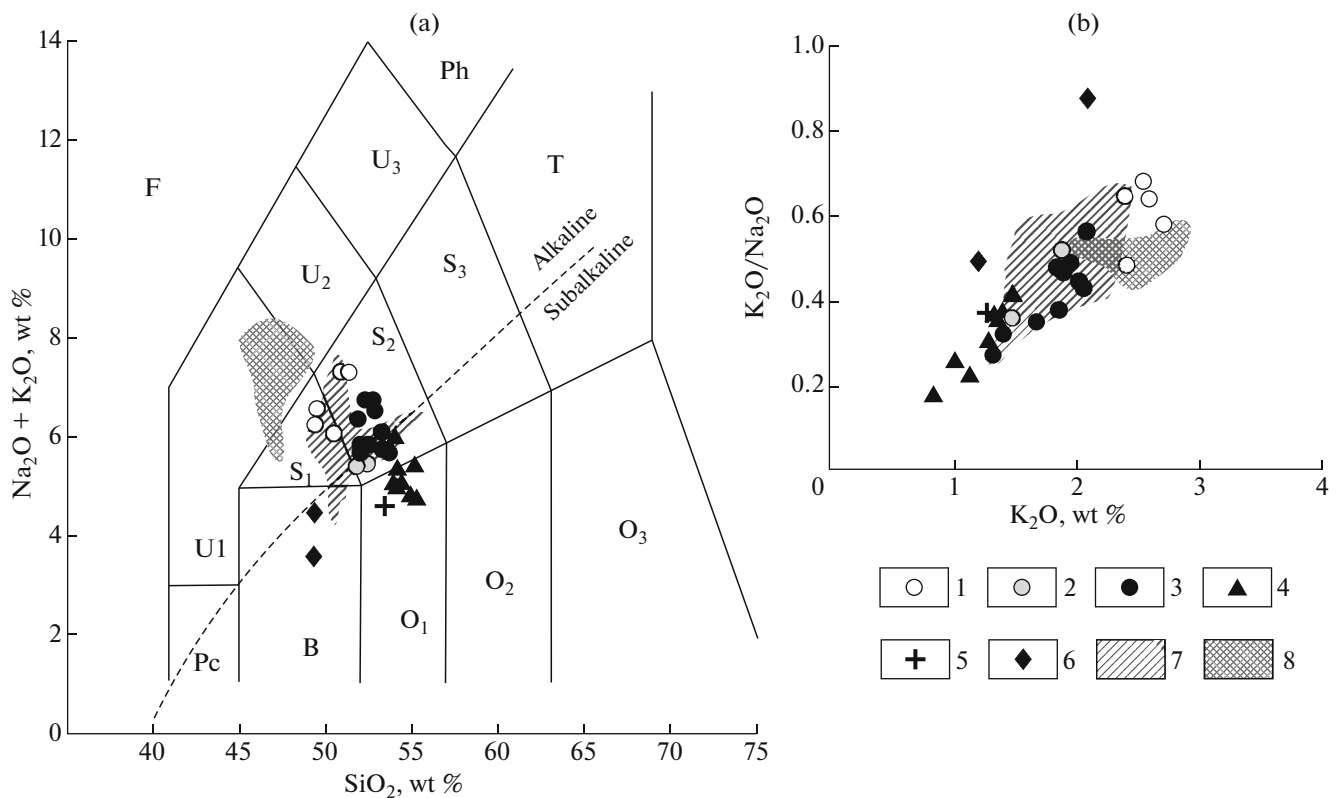


**Fig. 10.** Petrochemical characteristic of lavas and pyroclastics from Anyui Volcano.

(1–5) Anyui Volcano: (1) Flow I, (2) Flow II, (3) Flow III, (4) cinders and lava of the cone (Bazarova and Vavilov, 1989; Grachev, 1999; Ustiev, 1961) original data), (5) lavas of the parasitic cone (Dovgal and Chasovitin, 1965); (6) lavas from Bilibin Volcano (Chasovitin, 1966); (7) lavas of the Aluchin flow (Chasovitin, 1966; Gorodinskii et al., 1975; Grachev, 1999); (8) basalts from Balagan Tas Volcano (Grachev, 1999; Rudich, 1964; Vas'kovskii, 1949).

(a) TAS diagram (Le Bas et al., 1986): (F) foidites, (Pc) picrobasalts, (B) basalts, (O<sub>1</sub>) basaltic andesites, (O<sub>2</sub>) andesites, (O<sub>3</sub>) dacites, (R) rhyolites, (S<sub>1</sub>) trachybasalts, (S<sub>2</sub>) basaltic trachyandesites, (S<sub>3</sub>) trachyandesites, (T) trachytes and trachydacites, (U<sub>1</sub>) basanites and tephrites, (U<sub>2</sub>) phonotephrites, (U<sub>3</sub>) tephriphonolites, (Ph) phonolites. Line separating alkaline and subalkaline rocks, after (Irvine and Baragar, 1971).

are represented by trachybasalts and basaltic trachyandesites (Le Bas et al., 1986), while lavas and pyroclastics of the cinder cone (stage IV) are composed of basaltic andesites of normal alkalinity. Lavas are represented by different basalt varieties: Ne-normative (1.8–5.3%) variety of stages I and, partly, III; Hyp-normative variety of stage II; and Qtz–Hyp-normative basaltic andesites (Qtz 3.5–7.9%, Hyp 8.6–13.6%) of stage IV. The overcoming of the thermal barrier between the Ne-normative and Qtz-normative magmas in the low-pressure settings can be explained by the fractionation of magnetite-bearing mineral assemblages.

The peculiar feature of lavas from Anyui Volcano is the negative correlation between silica and alkali elements determined by changes in the K concentration (Figs. 10a, 10b). As a whole, lavas from this volcano are characterized by moderately high concentrations of Ti (TiO<sub>2</sub> = 1.46–2.23 wt %) and Fe (FeO<sub>tot</sub> = 7.3–9.6 wt %) and low contents of Al (Al<sub>2</sub>O<sub>3</sub> = 13.7–15.1 wt %).

The oxide–silica diagrams (Fig. 11), which include data points of the quenched glass in primary melt

inclusions (Bazarova and Vavilov, 1989), demonstrate generally negative correlations between TiO<sub>2</sub>, FeO<sub>tot</sub>, CaO, and K<sub>2</sub>O determined by the fractionation of clinopyroxene and plagioclase. The Na content in lavas is virtually independent from silica concentrations. The inclusion of data on melt inclusions into the analysis allows us to outline certain trends in magma differentiation during the separate effusive stages.

In the K<sub>2</sub>O–SiO<sub>2</sub> diagram (Fig. 11), rocks of Anyui Volcano make up three isolated areas represented by lavas of stages I, II–III, and IV demonstrating, in general, a negative correlation trend. At the same time, the composition of glasses from melt inclusions in lavas of eruption stage III (Bazarova and Vavilov, 1989) reflects a substantial increase in the K concentration against the background of increased silica contents. The similar trend is also observed in the Al<sub>2</sub>O<sub>3</sub>–SiO<sub>2</sub> diagram. As a whole, melt evolution during stage III was directed toward the increase in SiO<sub>2</sub>, Al<sub>2</sub>O<sub>3</sub>, and alkali contents, which resulted in the crystallization of K-feldspars in melt inclusions from olivine (Bazarova and Vavilov, 1989).

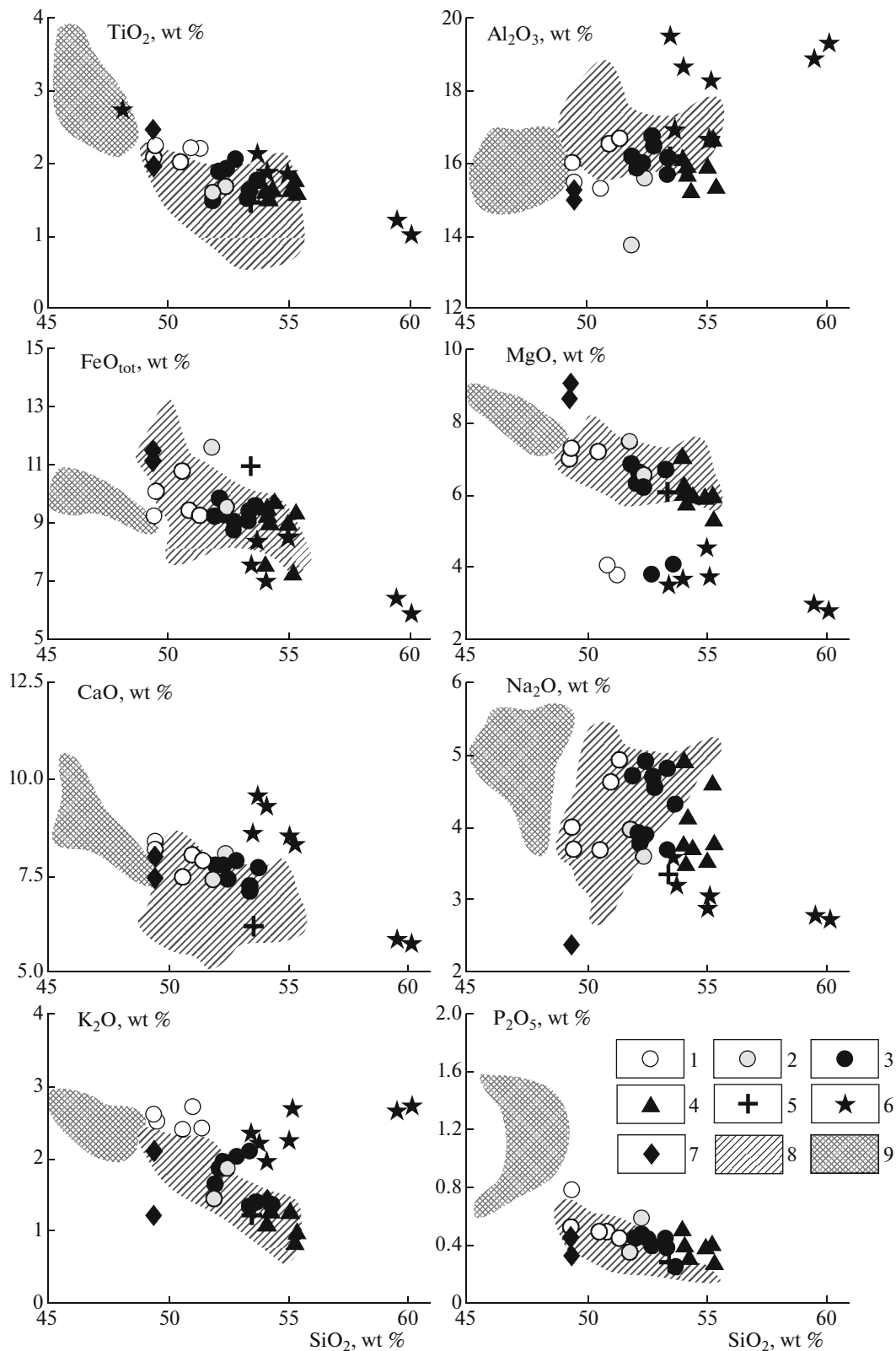


**Fig. 11.** Distribution of petrogenic elements (wt %) depending on the silica content in lavas and pyroclastics from Anyui Volcano. (1–6) Anyui Volcano: (1) Flow I, (2) Flow II, (3) Flow III, (4) cinders and lava of the cone (Bazarova and Vavilov, 1989; Grachev, 1999; Ustiev, 1961; original data), (5) lavas of the subsidiary cone (Dovgal and Chasovitin, 1965), (6) quenched glasses of melt inclusions in minerals of basaltic trachyandesites; (7) lavas from Bilibin Volcano (Chasovitin, 1966); (8) lavas from the Aluchin flow (Chasovitin, 1966; Gorodinskii et al., 1975; Grachev, 1999; Sakhno, 2001); (9) lavas from Balagan Tas Volcano (Grachev, 1999; Rudich, 1964; Vas’kovskii, 1949).

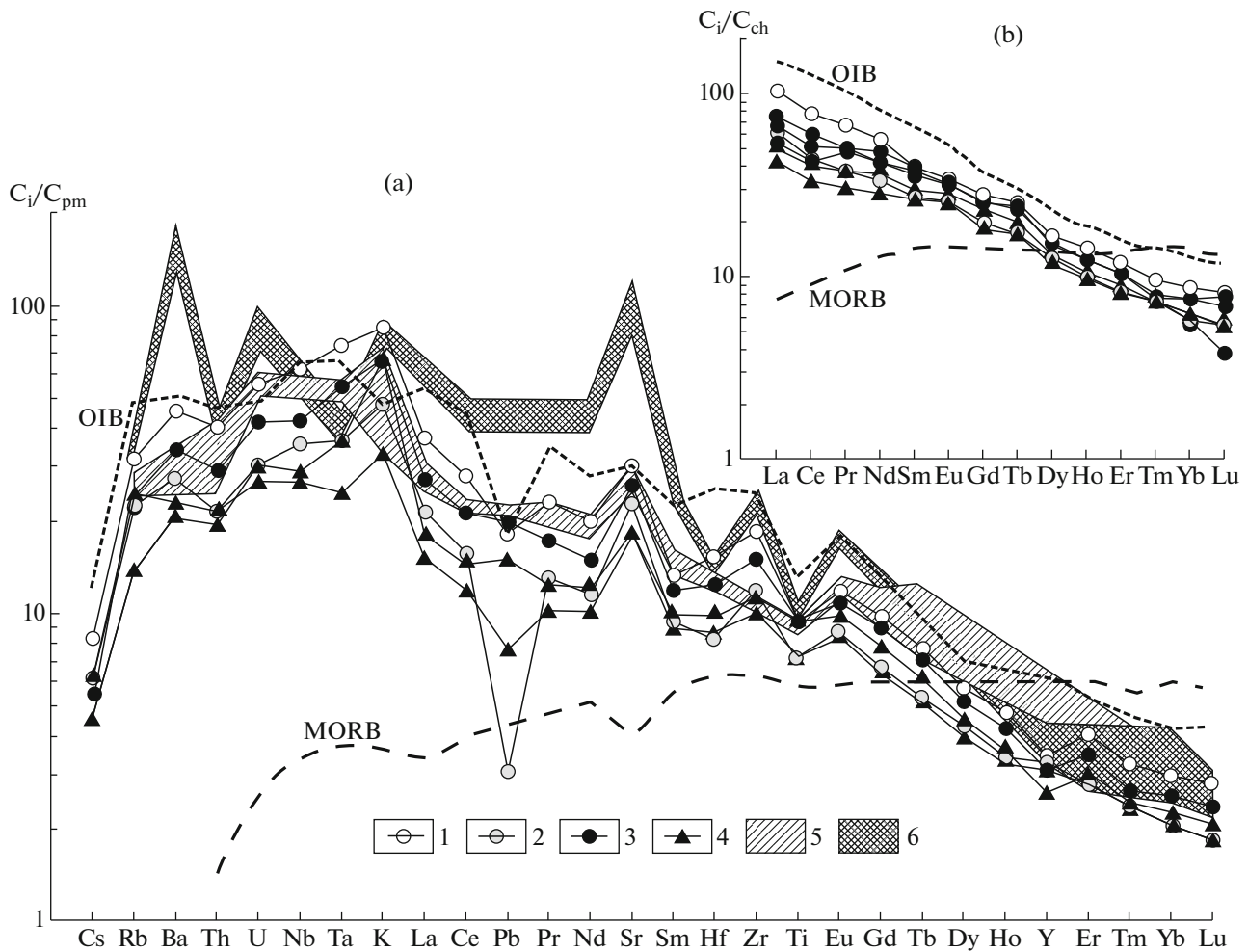


**Fig. 12.** Distribution of trace (a) and rare earth (b) elements in lavas from Anyui Volcano. (1–4) Anyui Volcano (Grachev, 1999; original data): (1) Flow I, (2) Flow II, (3) Flow III, (4) cinders and lava of the cone, (5) lavas from Aluchin Volcano (Grachev, 1999), (6) lavas from Balagan Tas Volcano (Grachev, 1999).

Comparison of the petrochemical composition of rocks from Anyui Volcano and lavas from Late Quaternary volcanoes in northeastern Russia demonstrates that they are, in general, close to lavas from Aluchin and, partly, Bilibin volcanoes, but notably differ from alkaline lavas of Balagan Tas Volcano (Figs. 10, 11).

The similarity and differences in the composition of rocks characterizing different stages of Anyui Volcano eruption are best seen in spidergrams (Fig. 12) based on the contents of incoherent elements normalized to the primitive mantle ( $C_i/C_{pm}$ ) (Sun and McDonough, 1989) and rare earth elements normalized to chondrite ( $C_i/C_{ch}$ ) (Evensen et al., 1978).

All rocks in Anyui Volcano are enriched with high field strength (HFSE) and large ion lithophile (LILE) elements as in intraplate basalts of oceanic islands (Sun and McDonough, 1989). They exhibit regular decrease in HFSE and LILE concentrations in the succession from basaltoids of eruption stage I to basaltic

andesites of the cinder cone (stage IV). These compositional properties are reflected in spidergrams by the appearance of Nb ( $Nb/Nb^* = 3-1$ )<sup>1</sup>, Ta ( $Ta/Ta^* = 4-1$ ), and Zr ( $Zr/Zr^* = 2.3-1.5$ ) maximums against the background of the Pb minimum ( $Pb/Pb^* = 0.9-0.2$ ) (Fig. 12a). Analysis of Th–Hf–Ta, Th/Yb–Ta/Yb, and other discriminant diagrams, which are missing in the figure, also supports the attribution of rocks from Anyui Volcano to intraplate basalts.

The REE distribution is fractionated (Fig. 12b). During the eruption,  $La_n/Sm_n$  and  $La_n/Yb_n$  values decrease successively: 2.7 and 11.9, respectively, in trachybasalts of stage I; 1.4–1.9 and 6.3–6.9, respec-

<sup>1</sup>  $Nb/Nb^*$  is a means to express Nb anomalies during the analysis of primitive mantle-normalized trace element concentrations. Nb is its measured content in rocks and  $Nb^*$  is its theoretical concentration calculated on the basis of the continuous spectrum of elements in neighboring spidergrams.  $Nb/Nb^* = Nb_n / [(Th_n) * (La_n)]^{1/2}$ .  $Zr/Zr^*$ ,  $Pb/Pb^*$ , and other anomalies are calculated in the similar way.

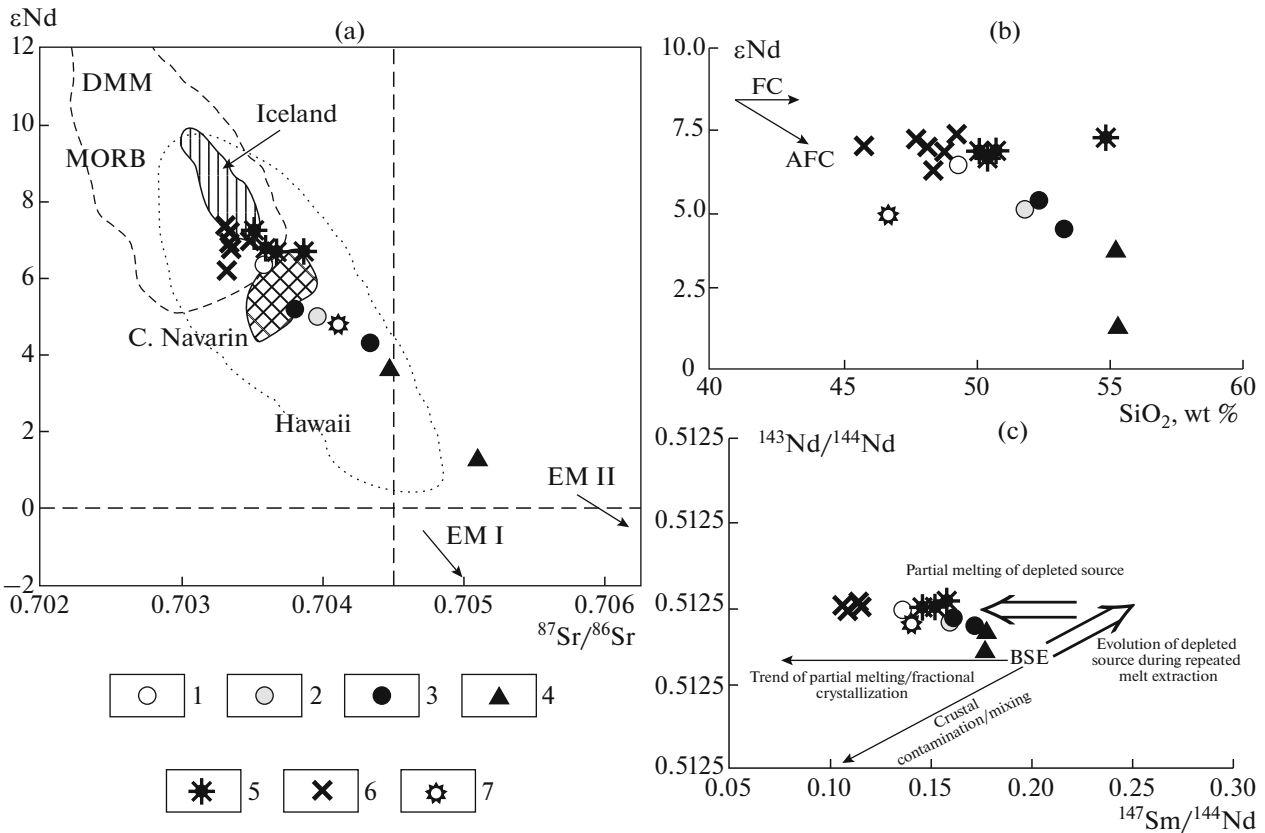


**Fig. 13.** Variations in isotopic and petrogenetic parameters in lavas from Anyui Volcano. (a)  $^{87}\text{Sr}/^{86}\text{Sr}$  and  $\epsilon\text{Nd}$  values. Fields of compositions of basalts from oceanic structures, after (Zindler and Hart, 1986) and Cape Navarin (Fedorov, 2006); (b)  $\epsilon\text{Nd}$  and  $\text{SiO}_2$  correlation. (FC) Fractional crystallization, (AFC) fractional crystallization and crustal contamination; (c)  $^{143}\text{Nd}/^{144}\text{Nd}$  and  $^{147}\text{Sm}/^{144}\text{Nd}$  correlation. Trends of variations in isotope ratios, after (Mukasa et al., 1996), (BSE) whole-rock isotopic composition of the Earth. (1–4) Anyui Volcano: (1) Flow I, (2) Flow II, (3) Flow III, (4) cinders and lava of the cone (Grachev, 1999; original data), (5) lavas from Aluchin Volcano (Grachev, 1999), (6) lavas from Balagan Tas Volcano (Grachev, 1999), (7) lavas from Pyatistennyi Volcano (Grachev, 1999).

tively, in basaltic andesites of the cinder cone (stage IV). Most rocks do not demonstrate Eu anomaly ( $\text{Eu}/\text{Eu}^* = 1.0\text{--}1.1$ ).

The ratio of Nd and Sm radiogenic isotopes in rocks of Anyui Volcano is highly variable (Fig. 13a). For example,  $^{87}\text{Sr}/^{86}\text{Sr}$  values are lower (0.703589) and  $^{143}\text{Nd}/^{144}\text{Nd}$  values are higher ( $\epsilon\text{Nd} = 6.4$ ) in trachybasalts of stage I than in basaltoids of stages II–III and lavas of the cinder cone (0.703796–0.705099 and 5.1–1.3, respectively). As a whole, Anyui basaltoids are characterized by more enriched Nd and Sr isotope composition as compared with lavas of Aluchin, Balagan Tas, and Pyatistennyi volcanoes. According to (Grachev, 1999), the high  $\text{He}^3/\text{He}^4$  values ( $0.15\text{--}18.0 \times 10^{-6}$ ) in lavas of Anyui Volcano are determined by their origination from three sources: depleted (MORB-type) mantle, mantle plume, and reworked oceanic crust.

The distinct negative correlation of  $\epsilon\text{Nd}$  with  $\text{SiO}_2$  (Fig. 13b) and positive  $^{87}\text{Sr}/^{86}\text{Sr}$  value (not shown in the

figure) indicate that magmas of the terminal eruption phase could be contaminated to some extent by the crustal material highly enriched with the radiogenic Nd. Contamination of mantle sources with material from the continental crust is quite probable, since basaltoids of Anyui Volcano were formed in an older continental crust 35–40 km thick. According to (Bazanova and Vavilov 1989), phenocrysts crystallized prior to the effusive period under the pressure of volatile elements amounting to approximately 700 MPa, which can correspond to a chamber depth of 20–25 km.

However, variations in the  $^{147}\text{Sm}/^{144}\text{Nd}$  values (Fig. 13c) in lavas from early stages of eruption are largely determined by the melting/fractional crystallization, while the crustal contamination could play some role only at terminal stages of magma generation. This is also confirmed by the location of the main eruptive center of Anyui Volcano within the Cretaceous Mount Vulkannaya quartz diorite massif (Miller et al., 2009).

The following scenario can be proposed for the formation of Anyui Volcano rocks on the basis of the obtained data.

The distinct negative correlation between  $K_2O$  and  $SiO_2$ , as well as Sr and Nd isotopic ratios, indicate at first sight that magma was generated in several sources. Such a scenario is well consistent with the compositional rock properties, but inconsistent with the real geological situation: lava erupted from a single eruptive center during a relatively short period (from a few months to a few years). In this connection, it is difficult to imagine a situation when magmas of different compositions could erupt from a single conduit during such a short time interval.

At early stages of eruption (Flow I), melting involved magmas relatively enriched in incompatible elements ( $(La/Sm)_n > 1$ ) and depleted in Nd ( $\epsilon Nd = 6.4$ ) and Sr ( $^{87}Sr/^{86}Sr = 0.703589$ ) isotopes, which produced Ne-normalized basaltoids. The subsequent increase in the degree of source matter melting and processes of contamination, which are reflected in the successive shift of the Nd and Sr isotope compositions ( $\epsilon Nd = 1.3$ ) and  $^{87}Sr/^{86}Sr = 0.705099$ ) in basaltic andesites of the cinder cone determined the compositional variety of rocks from Anyui Volcano. Such a scenario is close to some extent to the model of volcanism evolution on the Hawaiian Islands, where the alkali (underwater or pre-shield stage) volcanism was replaced by the tholeiitic (shield stage) volcanism that continued for approximately 50 Ma (Clague, 1987; and others).

It may be assumed that magma chamber feeding Anyui Volcano acted as a “running system;” i.e., upon reaching a certain degree of fractionation, the melts mixed with the next portion of primary melt, which resulted in the eruption of mainly products of their differentiation and mixing with residual melts in the chamber (Kadik et al., 1990). Such a scenario is admissible only in situation when stratigraphic succession of the defined eruption stages is ignored.

Summing up, the following should be noted. Rocks of Anyui Volcano are represented by moderately magnesian subalkali trachybasalts, basaltic trachyandesites, and basaltic andesites. The reconstructed succession of lava eruptions and exact placing of sampled rocks in this succession made it possible to reveal the general basic-to-acid trend in the volcanism evolution. The peculiar feature of melt evolution is a distinct negative correlation between K and  $SiO_2$  concentrations. The isotopic-geochemical composition of basaltoids of Anyui Volcano implies their formation by the partial melting of a source depleted in isotopes (Nd–Sr) and enriched in incoherent elements with a simultaneous contribution of crustal contamination. Such an inconsistency between the isotopic and trace element compositions of magmas could be determined by the preceding Mesozoic metasomatic events.

## RESULTS OF RADIOMETRIC DATING

Taking into consideration the high degree of morphological preservation of the well-exposed lava flow and cone, which lack any features indicating the influence of glacial activity on them, Ustiev (1961) assumed that Anyui Volcano was formed a few centuries ago. Most researchers share this view on its age and attribute its formation at least to the Holocene (Akinin et al, 2008; and others). They mention evidence of local residents who supposedly witnessed smoke above the volcano (*Geologicheskaya ...*, 1979). Based on its relations with glacial forms, some researchers assumed its late Sartanian age (Ignat’ev, 1990; Sizykh, 1993; Ignat’ev and Sizykh, 2001). In some publications (Surnin, 1997; Surnin et al., 1998), it is indicated that the age of Balagan Tas and Ustiev volcanoes is 0.2–0.4 Ma, although the authors give no information on the initial isotopic date or corresponding references. In (Akinin and Calvert, 2012), the age of Anyui Volcano is estimated to be  $42.7 \pm 2.4$  and  $12.9 \pm 3.4$  ka ( $^{40}Ar/^{39}Ar$  method, US Geological Survey). According to our isotopic measurements (K–Ar method, GIN RAN), Anyui Volcano was formed approximately 250 ka ago ( $0.248 \pm 0.030$  Ma) (Pevzner et al., 2011).

### *Radiocarbon Dating*

The tephrochronological method is used worldwide for determining the age of volcanic eruptions (Lowe, 2011). In Russia, the tephrochronological dating of Holocene eruptions and associated deposits are conducted in Kamchatka since the 1970s (Braitseva et al., 1978a, 1978b) and now this method is successfully used in geological investigations. It is based on the detection and dating of ejected tephra in isolated sections using simultaneously both tephrostratigraphic data and results of the immediate radiocarbon dating of pyroclastics from organogenic sediments. The presence of the large cinder cone of Anyui Volcano implies ejections of relatively large volumes of tephra, which should be spread and accumulate in unconsolidated sediments over dozens of kilometers from the crater. The study area is located substantially far from the centers of volcanism. Therefore, we could not use additional tephrochronological reference levels (previously dated transit ashes of other volcanoes) and were forced to apply the only possible approach: immediate dating of tephra buried in sediments enriched with organic matter, i.e., in peatlands.

The high degree of cinder cone destruction (mainly, absence of unconsolidated black cinder on slopes of the cone and strong destruction of its northwestern part) and complete absence of pyroclastic sediments in the study area forced us to doubt the Holocene age of the eruption under consideration. Nevertheless, we sampled near Lake Kukol several sections of Holocene peatlands, which were related to damming of the Monni River valley by lavas. The sections are located

**Table 3.** Results of the radiocarbon dating of peatlands

Sample no.		Sampling site (distance from the cone)	Material	<sup>14</sup> C date, yr
lab	field			
GIN-14104	0911-A1	Southeastern coast of Lake Kukol, peat 1.8 m thick on frost talus (3.5 km)	Detritus from depth 1.6 m	2860 ± 40 dt 3270 ± 30 h
GIN-14105	0912-A1	Northwestern coast of Lake Kukol, peat 1.4 m thick on frost talus (3.8 km)	Peat from depth 1.4 m	4880 ± 60 h1 4670 ± 40 h2
GIN-14116	31/09	Eastern coast of Lake Kukol, peat 1.2 m thick on frost lacustrine–fluvial sediments (3.7 km)	Peat from depth 1.2 m	1620 ± 30 h
GIN-14117	32/09	The same	Peat from depth 0.49 m	970 ± 30 h
GIN-14118	53/09	Bol'shoi Keperveem River, upstream of Bilibino, peat 2.0 m thick on alluvial pebble gravel (100 km)	Peat from depth 2.0 m	8460 ± 40 h
GIN-14119	54/09	The same	Peat from depth 1.7 m	6980 ± 40 h

Dates are derived from humic alkaline extractions: (h1) first cold, (h2) second hot, (h) only hot, and (dt) from plant detritus.

4 km away from the cinder cone and their location seems to be an ideal “trap” for volcanic ash, which should fall during the formation of the cone. The presumable thickness of tephra at such distance (by analogy with tephra of Southern breakthrough of the Great Fissure Tolbachik Eruption (*Bol'shoe* ..., 1984) should amount to decimeters and not less than 0.1 m. At the same time, none of these sections and their more remote counterparts contain any traces of cinder or other pyroclastics even in the reworked state.

The basal part of the continuous peatland located 3.8 km away from the cinder cone yielded radiocarbon date of 4880 ± 60 <sup>14</sup>C yr (Table 3). The peat represents a virtually ideal substrate for the burial of falling tephra. The absence of any traces of pyroclastic material or ballistic ejecta, which is related to explosive activity of the cinder cone of Anyui Volcano in the examined section, indicates unambiguously that the eruption took place about 5600 cal. yr ago. The radiocarbon age was recalculated into the calendar one in accordance with (Bronk Ramsey, 2005).

Inasmuch as organic matter in this area commenced to accumulate only during the Holocene climatic optimum, the obtained date implies severe climatic conditions at that time. Other samples from the basal part of the continuous peatland sections located up to 4 km away from the cone yielded even younger dates (Table 3). The milder climate in the Keperveem River valley (outskirts of the town of Bilibino) is evident from the date of 8460 ± 40 <sup>14</sup>C yr ago (Table 3) that was also obtained for the basal part of the continuous peatland 2 m thick. This section located approximately 100 km away from the cone also lacks any traces of tephra produced by Anyui Volcano. Unfortunately, we failed to find older peats. Nevertheless, even the obtained dates refute the myth about the “historical” age of the eruption. Radiocarbon ages were measured in the Chemical-Analytical Laboratory of GIN RAN in accordance with the standard technique.

### *K–Ar Dating*

Field observations on the volcano in question provided grounds for assuming relatively old age for its eruption and rocks sampled for the K–Ar dating. The rock collection included lavas from earliest Flow I (samples 0914/1, 0916/2) and younger Flow III<sub>2</sub> (samples 0909/1, 0913/1). The samples were taken 0.2 to 4.8 km away from the cinder cone. Lavas are represented by the high-K Pl–Ol basalts with the content of phenocrysts ranging from 10 to 20% except for sample 013/1 characterized by the aphyric texture. Table 4 illustrates the results of measurements.

Concentrations of the radiogenic Ar were measured in samples weighing 160–190 mg in the Chemical-Analytical Laboratory of GIN RAS with an MI 1201 IG mass spectrometer by the isotope dilution method using <sup>38</sup>Ar monoisotope. Samples were melted at 1500°C. Gas was cleaned on the trap cooled by ethanol at –121°C and then on two steps of Ti–Zr–Al getter. Errors in measurements of the radiogenic Ar content and sample age were calculated in accordance with the technique in (Chernyshev et al, 2006) with account of their maximum values. The K concentrations were measured on an AAS3 atomic absorber in the Chemical-Analytical Laboratory of GIN RAS with an accuracy of <1% (analyst I.V. Kiseleva). Validity of the obtained results was controlled by the consistency between repeated measurements and reproducibility of analyses of standard samples. The following constants were used in calculations:  $\lambda_e = 0.581 \times 10^{-10} \text{ yr}^{-1}$ ;  $\lambda_\beta = 4.962 \times 10^{-10} \text{ yr}^{-1}$ ; and  $^{40}\text{K}/\text{K} = 1.167 \times 10^{-4}$  (Staiger and Jager, 1977).

The K–Ar method is usually used for the dating of rocks millions of years old. However, when large weights of ideally preserved samples with high K contents are analyzed on the preliminarily prepared mass spectrometer, it may also be applied for the dating of younger rocks. For example, the report on ages obtained by both the isotopic (<sup>14</sup>C, K–Ar, <sup>40</sup>Ar/<sup>39</sup>Ar, <sup>230</sup>Th/<sup>238</sup>U) and thermoluminescence (TL) methods is

**Table 4.** Results of the K–Ar dating of lavas from Anyui Volcano

Lab no.	Sample no., sampling coordinates	K, wt %	$^{40}\text{Ar}$ rad, $\text{nmm}^3/\text{yr} \pm \sigma$	$^{40}\text{Ar}$ atm in sample, %	Age, Ma
GIN-31	0909/1 N 67°11'14.4" E 165°51'22.3" h 725	1.42	$130 \times 10^{-7} \pm 33$	97.2	$0.236 \pm 0.065$
			$132 \times 10^{-7} \pm 18$	94.5	$0.238 \pm 0.040$
			$138 \times 10^{-7} \pm 18$	94.2	$0.249 \pm 0.040$
GIN-55	0913/1 N 67°11'46.7" E 165°51'34.6" h 602	1.08	$98 \times 10^{-7} \pm 53$	98.7	$0.234 \pm 0.130$
			$85 \times 10^{-7} \pm 38$	98.4	$0.228 \pm 0.110$
GIN-56	0914/1 N 67°12'39.9" E 165°49'16.2" h 501	1.74	$185 \times 10^{-7} \pm 15$	90.5	$0.273 \pm 0.030$
			$173 \times 10^{-7} \pm 15$	91.0	$0.255 \pm 0.030$
GIN-58	0916/2 N 67°10'52.0" E 165°50'30.6" h 827	1.65	$159 \times 10^{-7} \pm 23$	95.0	$0.248 \pm 0.045$
			$173 \times 10^{-7} \pm 22$	94.2	$0.270 \pm 0.040$

available for the young Olbi and Lachampe basaltic flows (France) (Plenier et al., 2007; Singer et al., 2009). Age of these flows is estimated to be approximately 36 ka: 31–43 ka (TL method); 40–42 and 47 ka ( $^{40}\text{Ar}/^{39}\text{Ar}$  method); and 39 ka ( $^{230}\text{Th}/^{238}\text{U}$  method). K–Ar dates fall into the time interval of 33 to 45 ka: 38–45 ka (Cassignol and Gillot, 1982) and 33–41 ka (Plenier et al., 2007). This example of cross dating illustrates perfectly the potential of the K–Ar method for measurements of the age of young rocks. However, when we are dealing with Middle–Late Pleistocene samples, application of alternative methods is desirable.

In the situation under consideration when the alternative dating is impossible, we paid significant attention to properties of lavas sampled for isotopic investigations. In order to exclude probable losses of the radiogenic argon, we sampled lavas with the minimum quantity of pores and without traces of oxidation or repeated overheating. In laboratory, the lavas were examined in thin sections. The equipment was preliminarily prepared for the work with young samples: the mass spectrometer sensitivity was substantially increased, the device for Ar cleaning was tested, and the mass spectrometer chamber was cleaned from the possible traces of previous samples. For measurements, large weights of samples with different K contents were used (Table 4).

Accuracy in measurements of the radiogenic argon concentrations based on consistency between the data on different weights was approximately 2%. The final error ( $\sigma$ ) presented in Table 4 was calculated in accordance with the technique in (Chernyshev et al, 2006) based on integral errors in the measurement of Ar and K, as well as errors in calculations of the  $^{40}\text{K}$  radioac-

tive decay constant and increase of calculation error due to the large share of atmospheric argon.

Proceeding from the above-mentioned data, age of the Anyui Volcano formation can be estimated as  $0.248 \pm 0.030$  Ma. It is noteworthy that the radiometric date obtained by the  $^{40}\text{Ar}/^{39}\text{Ar}$  method for lavas of Balagan Tas Volcano in Yakutia is  $0.266 \pm 0.030$  Ma (Leier et al., 1993). Moreover, both volcanic edifices (Anyui and Balagan Tas) are characterized by a similar degree of preservation of their cinder cones.

## ASSESSMENT OF THE ERUPTION AGE

### *Discussion of Radiometric Dating Results*

After publication of the article (Pevzner et al., 2011), in which age of Anyui Volcano was estimated to be approximately 250 ka, new  $^{40}\text{Ar}/^{39}\text{Ar}$  dates were reported in (Akinin and Calvert, 2012), according to which Anyui Volcano was formed in the Holocene. In the last work, three samples taken for dating were mentioned, but only two dates ( $42.7 \pm 2.4$  and  $12.9 \pm 3.4$  ka), which was obtained for samples from the cinder cone crater, and “lava flow extending from the latter in the Monni River valley” are presented (Akinin and Calvert, 2012, p. 25). Tables with particular dates and plateau plots are also missing.

In our opinion, these dates and corresponding inferences are inconsistent with the real geological situation. First, the dates cannot characterize the Holocene age. The lower limit for the Holocene is accepted at  $11700 \pm 99$  ka (*Stratigraficheskii ...*, 2006; *The 2016 Version ...*, 2016). Second, our observations on Anyui Volcano give reasons for doubts in the possibility of obtaining valid dates for rocks in the cone edifice, since they are mostly overheated and strongly oxi-

dized. Even on lava flows, we met significant difficulties in sampling for the radiometric dating: individual portions of lava are usually very thin and have distinctly overheated contact zones (Fig. 7). Even oxidized lavas contain abundant pores, which prevent their K–Ar and  $^{40}\text{Ar}/^{39}\text{Ar}$  dating.

In addition to dates on Anyui Volcano, Akinin and Calvert (2012) also cite the first radiometric ( $^{40}\text{Ar}/^{39}\text{Ar}$ ) date for lavas of the Aluchin flow, which is located 80 km southward. According to their data, Aluchin Volcano was formed  $277.3 \pm 2.1$  ka ago.

Figure 14a shows that the dates obtained for Balagan Tas ( $^{40}\text{Ar}/^{39}\text{Ar}$ ) and Anyui (K–Ar) volcanoes are characterized by the confidence interval of 30 ka, which is approximately equal to 12% of the measured age value. The  $^{40}\text{Ar}/^{39}\text{Ar}$  date obtained for the Aluchin flow is characterized by the confidence interval of 2.1 ka, which constitutes <1% (0.76%) of the measured age value. In our opinion, these accuracy values for the date, which determines the *stratigraphic* age of such young rocks, seem to be unreal. We assume that the mentioned confidence interval is based on similarity between the data on two weights from the same sample rather than standard deviation ( $\sigma$ ). When calculating errors in the Ar–Ar dating, the researcher usually takes into consideration both errors in calculations of the  $^{40}\text{K}$  radioactive decay constant and accuracy of K/Ca measurements. If the confidence interval of 30 ka (approximately 11%) is accepted for the date under consideration, it is possible to define based on three available dates (Fig. 14a) a common field of the overlapping confidence intervals (280–250 ka) and consider this date as corresponding to age of the Middle Quaternary volcanism impulse in northeastern Russia. Even taking into consideration the scarcity of available factual material (only three dates), such an accuracy in age determination appears to be relatively high.

Let us consider  $^{40}\text{Ar}/^{39}\text{Ar}$  dates obtained for Anyui Volcano (Fig. 14b). The confidence intervals for these dates are large (19 and 26%). However, they demonstrate no overlapping! The gap between these dates is 24–30 ka; i.e., two dates obtained by the same method for the same object are inconsistent with each other. Such a discrepancy in dates is possible only in the case of dating heterochronous events. However, when considering the above-mentioned structural features and succession of Anyui Volcano eruption, we established that we are dealing with a normal monogenic center, which could be maximum active during several years. Consequently, at least one of the obtained dates ( $42.7 \pm 2.4$  or  $12.9 \pm 3.4$  ka) is incorrect because of the fivefold excess of  $\sigma$ .

Unfortunately, primary data, including plateau plots (data on Ar release), diagrams of measured K/Ca values, and isochrones, which served as a basis for calculating such young ages in (Akinin and Calvert, 2012), have not been published so far. It is quite likely that different steps of the plateau also include steps

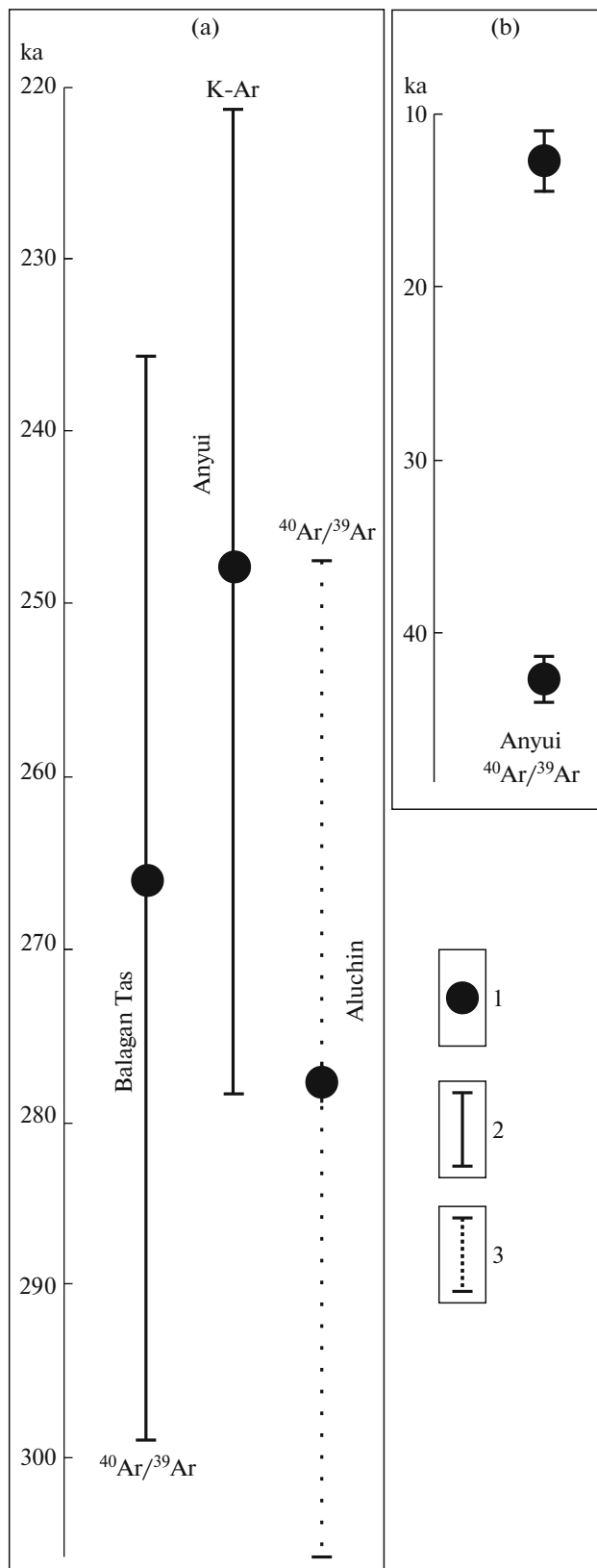


**Fig. 14.** Radiometric dates for Balagan Tas (a), Aluchin (b), and Anyui (a, b) volcanoes. (1) Age; (2, 3) confidence interval: (2) accepted, (3) proposed.



corresponding to values ranging from 280 to 250 ka, and the choice of youngest dates (plateau steps with the overstated content of atmospheric  $^{40}\text{Ar}$ ) could be related to the relatively young appearance of lava flows of Anyui Volcano and traditional view on the Holocene age of this eruption. In addition, it should also be taken into consideration that the preceding impulse of magmatic activation is recorded in the continental part of Chukotka in the Cretaceous (Miller et al., 2009). In this connection, it can hardly be expected that eruptions in the Late and Middle Holocene became frequent.

The degree of preservation of volcanic morphostructures, as well as distinct morphological features of flows and cones, cannot necessarily serve as unambiguous criteria for estimating the age of volcanic edifice. We meet frequently such problems in Kamchatka (Pevzner, 2015). In areas remote from most sources of Holocene eruption, primary morphostructures of lava flows are very slowly covered by sediments. Kamchatka avoided shield glaciation in the terminal Late Pleistocene, while mountain valley glaciers occupied only some centers. In this connection, many volcanic objects may *look* young, which lead frequently to substantial underestimation of their age. Anyui Volcano surrounded by the Triassic and Cretaceous mountains look naturally *relatively* young: it includes the cinder cone with the preserved crater; its lava flows are exposed and bear no indications of glacial abrasion. Nevertheless, the reliable age of eruptions and their associated products is determinable not only on the basis of radiometric dating, but also different geochronological methods with account for the general geological evolution of the region.

#### *Age and Parameters of the Last Glaciation in the Study Area*

Most researchers consider the last, Sartanian glaciation in Chukotka as being represented by cirque glaciers, which developed similarly to the North Yakutia type (*Dinamika* ..., 2002; Elias and Brigham-Grette, 2013; Glushkova, 1984, 2001; *Poyasnitel'naya* ..., 2013; Pushkar and Cherepanova, 2011; *Razvitie* ..., 1993; Verkhovskaya, 1986; and others). The glaciation of the North Yakutia type is determined by the moisture deficiency, which hampers the formation of large land glaciers. The moisture deficiency could result from desiccation of the northern shelf of eastern Asia over 300–700 km along the northern direction and the Bering Sea over 600–850 km south of the Chukchi Peninsula (Laukhin et al., 2006). Glushkova (1996) defined the mountain valley glaciation only in some areas of the Okhotsk region.

The Zyryanka glaciation was significantly larger as compared with the Sartanian one. Nevertheless, its moraines were established and dated only in mountains surrounding Chukotka rather than in its central part (*Poyasnitel'naya* ..., 2013). It is established that pied-

mont plains of the Verkhoyansk Range accumulated continuously periglacial sediments during the last 60 ka in extremely continental climatic environments, which are responsible for the absence of substantial mountain glaciations at that time (Zigert et al., 2007).

Glaciomarine sediments are recorded in the Selezha and Berelekh river basins (Okhotsk region) and south of Cape Dionisiya (Anadyr area). Their age is estimated at 150 ka based on the date of  $148 \pm 40$  ka obtained by the thermoluminescence method (*Poyasnitel'naya* ..., 2013).

The oldest moraine is documented in the Yurovka River basin (Okhotsk region). It is dated at  $250 \pm 50$  ka by the thermoluminescence method (*Poyasnitel'naya* ..., 2013).

Since 1998, bottom sediments of Lake El'gygytyn located 270 km north-northeastward of Anyui Volcano are investigated by drilling. These comprehensive investigations revealed that the area in question was characterized during the last 300 ka by continuous sedimentation in the lacustrine depositional environment with seasonal ice cover, while the surrounding areas were free of large glaciations (Lozhkin et al., 2007; Melles et al., 2012; Shilo et al., 2001). No tephra of Anyui Volcano was detected in sediments of Lake El'gygytyn (Van den Bogaard et al., 2014).

The cinder cone of Anyui Volcano is located in a large complex collapse cirque on the northern slope of Mount Vulkannaya (Figs. 2, 3). It is quite probable that the collapse was caused by seismic processes during the magma ascent. At the same time, southern slopes of Mount Vulkannaya and other surrounding mounts lack such distinct erosional morphostructures. The detachment wall of the collapse cirque is almost vertical and about 500 m high. Its lower part is buried under talus with inclination amounting to  $35^\circ$ . The rockslide body composed of large (up to 3 m across) blocks of granitoids (quartz diorites) forms "giant steps" descending in a northerly direction. Blocks are spread over a maximum distance of 3 km away from the cone. Locally, it is well seen that lavas overlie accumulations of large rock blocks. These blocks bear no indications of glacial abrasion. Their facets are only slightly affected by other rock fragments, which is characteristic precisely of rockslide deposits. The rockslide body proper is poorly recognizable, which indicates, first, its virtually complete burial under lavas of Anyui Volcano, and, second, pre-Holocene age of the event. Nevertheless, the "steps" are very distinct, which probably determined to a significant extent the stepped profile of the lava flow descending in a northerly direction.

As was noted (Ustiev, 1958a,b, 1961, 1966), fragments of diorites occur frequently both on the surface of the lava flow and inside the crater. They are most widespread near bedrock slopes, on lavas near the cone, and at a distance up to 1.5 km away from the latter. The fragments never exceed 1 to 2 m across (dominant size

up to 0.6 m) on lavas and 0.3 m inside the crater. Rock fragments in the crater are strongly affected by the interaction with other blocks. They are characterized by relatively acute facets and could most likely roll down from slopes of Mount Vulkannaya when the cone leaned against the latter. Blocks could appear on the flow owing to both roll down from the slopes and mudflow transportation. Development of mudflows is evident from the structure of the creek channel incised into Flow III<sub>2</sub> to a maximum depth of 3 m (Fig. 7).

The cinder cone is located between two well-developed isometric depressions filled with proluvium (Figs. 3, 8). Their bottoms are flat and covered by turf and incipient frost polygons. These depressions can also be interpreted as cirques. Some researchers (Ignat'ev, 1990, 1993; Ignat'ev and Sizykh, 1997) define glacial morphostructures (cirques and even moraine) near the cone of Anyui Volcano. The moraine is considered by these authors as the Sartanian deposit. They also emphasize its insignificant volume. This is explained, in turn, by the insignificant ice thickness in cirques. We failed to find any indications of glaciation larger than the cirque mentioned by these researchers (Ignat'ev and Sizykh, 1990, 1993, 1997). We believe that relatively good preservation of the cinder cone and lava flow of Anyui Volcano is explained by the absence of such glaciation.

The formation of Anyui Volcano (~250 ka ago) is chronologically close to the boundary between isotopic stages 7 and 8 (Bradley, 1985). The paleogeographic data derived from drill core recovered from Lake El'gygytyn indicate that cooling during Stage 8 and the later cooling event (isotopic stages 2, 4, 6) were characterized by the dry or even arid climate (Lozhkin et al., 2007). Thus, the lack of indications of a substantial influence of glaciers on volcanic deposits can be interpreted as their absence in the area under consideration at least during the last 250 ka. Our inference on the absence of shield or large mountain valley glaciations in the continental part of Chukotka is consistent with most available observations.

*Eruption of Anyui Volcano against the Background of Pliocene–Quaternary Volcanic Activity in the Arctic and Subarctic Regions*

Studies in all volcanic domains of the world are aimed at dating of eruptions. These investigations provided extensive data, which made it possible to reveal episodes of volcanism activation in some regions. Different detailed reports on volcanic activity over the last 3–6 Ma are available for the Arctic and Subarctic regions: Iceland and Yan Mayen (Lacasse and Garbeschoonberg, 2001); Spitsbergen Archipelago and Novaya Zemlya (Akinin et al., 2008; Vaganov et al., 1985); Gakkel Ridge (Sohn et al., 2008); De-Longa Archipelago (Bogdanovskii et al., 1992; Leier et al., 1993; Zaitsev et al., 2011); and Alaska and northwestern Canada (Yukon) (Edwards and Russell, 2000;

Jackson et al., 2001; Moll-Stalcup, 1994; Mukasa et al., 2007). In the North Pacific, tephra intercalations were studied in the ODP Holes 883 (Kamchatka arc), 887 (Aleutian arc), and other sections, which made it possible to reveal episodes of explosive volcanism and establish age of the largest events at least at the regional scale (Prueher and Rea, 2001).

The schematic profile extending from Iceland to Alaska illustrates post-Miocene volcanic activity in the Arctic region. Volcanic episodes in the continental part of northeastern Russia are united into a single column in this profile (Fig. 15). The strongest volcanism episodes in the North Pacific (Prueher and Rea, 2001) are shown conditionally (between columns characterizing volcanic activity in Kamchatka and Aleutian Islands). Comparison of the chronological succession in volcanic activity of the Arctic region, North Pacific, and Atlantic Ocean indicates that the entire region under consideration was characterized by intensified volcanic activity likely in response to global events approximately 0.3, 0.8, 1.7, and 2.6 Ma ago.

In this connection, it is logical to assume that Middle Quaternary volcanic activation in Chukotka (Anyui and Aluchin volcanoes) and Yakutia (Balagan Tas Volcano) was determined by the “repercussion” of global processes. In such a situation, it becomes clear that ages of the eruptions of Anyui, Aluchin, and Balagan Tas volcanoes should be similar (it has been established) or differ at least by 0.5 Ma. It is quite probable that the age of Bilibin Volcano, which belongs to the Anyui group of volcanoes should fall into the interval of 0.2–0.3 Ma or correspond to earlier episodes defined in (Prueher and Rea, 2001). It would also be of interest to determine the age of Pyatistennyi Volcano located within the South Anyui suture 200 km north-northwest of the Anyui group (Fig. 1).

Among other Quaternary volcanoes of northeastern Russia, relatively reliable age estimates were obtained for volcanics of Cape Navarin (1.45–1.59 Ma) (Koloskov et al., 1992). Their age is well consistent with the episode of volcanic activation in the Kamchatka segment of the North Pacific (1.5–1.7 Ma ago) defined in (Prueher and Rea, 2001) and with the subsynchronous episode of volcanism activation in Alaska (Edwards and Russell, 2000; Jackson et al., 2001; Moll-Stalcup, 1994; Mukasa et al., 2007). Many Pliocene–Quaternary eruptions have been established and dated in Zhokhov and Vil'kitskii islands (De-Longa Archipelago, Fig. 1). The last eruptions are dated at 0.4 and 0.5 Ma ago (Bogdanovskii et al., 1992)).

Figure 15 demonstrates clearly that the continental part of northeastern Russia looks passive among the majority of active areas in the Arctic and Subarctic regions. In this connection, the established age of three volcanic centers (Anyui, Aluchin, and Balagan Tas) is extremely important, since it allows the last episode of volcanic activation 0.2–0.3 Ma ago to be confidently defined for the continental part of this

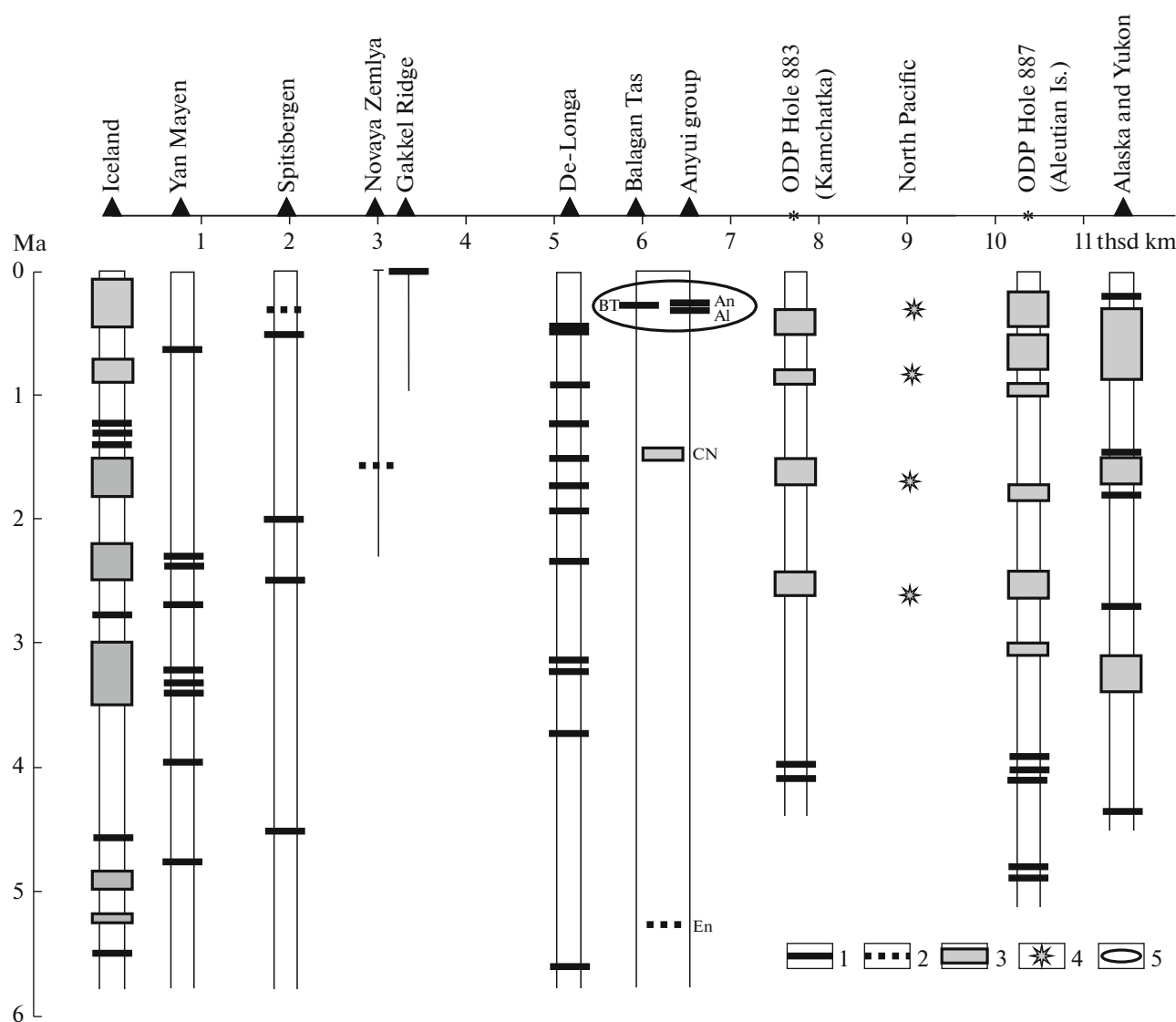


**Fig. 15.** Episodes of volcanism activation in the Arctic region and adjacent areas during the Pliocene–Quaternary shown on the composite profile. In inset, schematic location of columns from the composite profile in the map of earthquake epicenters in the Arctic and Subarctic regions (Avetisov, 1996).

(1, 2) Single eruptions: (1) reliably dated, (2) with approximate stratigraphic age; (3) episodes of intensified volcanic activity; (4) strongest volcanism outbursts in the North Pacific; (5) last episode of volcanism activation in the continental part of northeastern Russia.

Volcanoes: (An) Anyui, (BT) Balagan Tas, (Al) Aluchin, (CN) Cape Navarin, (En) Enmelen.

Columns: Iceland and Yan Mayen (Lacasse and Garbe-Schoonberg, 2001), Spitsbergen Archipelago and Novaya Zemlya (Akinin et al., 2008; Vaganov et al., 1985), Gakkel Ridge (Sohn et al., 2008), De-Longa Archipelago (Bogdanovskii et al., 1992; Leier et al., 1993; Zaitsev et al., 2011), northeastern Russia (Akinin et al., 2008; Akinin and Calvert, 2012; Leier et al., 1993), North Pacific (strongest) (Prueher and Rea, 2001), Alaska and northwestern Canada (Yukon) (Edwards and Russell, 2000; Jackson et al., 2001; Moll-Stalcup, 1994; Mukasa et al., 2007), Aleutian arc Borehole 887 (Prueher and Rea, 2001), Kamchatka arc Borehole 883 (Prueher and Rea, 2001). In the inset: (A) Anyui group of volcanoes, (B) Balagan Tas, (G) recent eruptions in the Gakkel Ridge, (N) volcanoes of Cape Navarin, (E) Enmelen volcanoes.

region. If the youngest eruptions in the De-Longa Archipelago are taken into consideration, the chronological limit of this episode for the entire northeastern Russia region corresponds to the interval of 0.2–0.5 Ma. Noteworthy is the fact that volcanic activity at that time was characteristic of the entire periphery of the Arctic and Subarctic regions (Iceland,

Spitsbergen, Kamchatka, Aleutian Islands, and Alaska) (Fig. 15), which indicates both significant scale and high intensity of this phenomenon.

Given that volcanism of continental Chukotka is indirectly associated with global impulses of volcanism, the next eruption in northeastern Russia may be expected not earlier than 0.2–0.5 Ma.

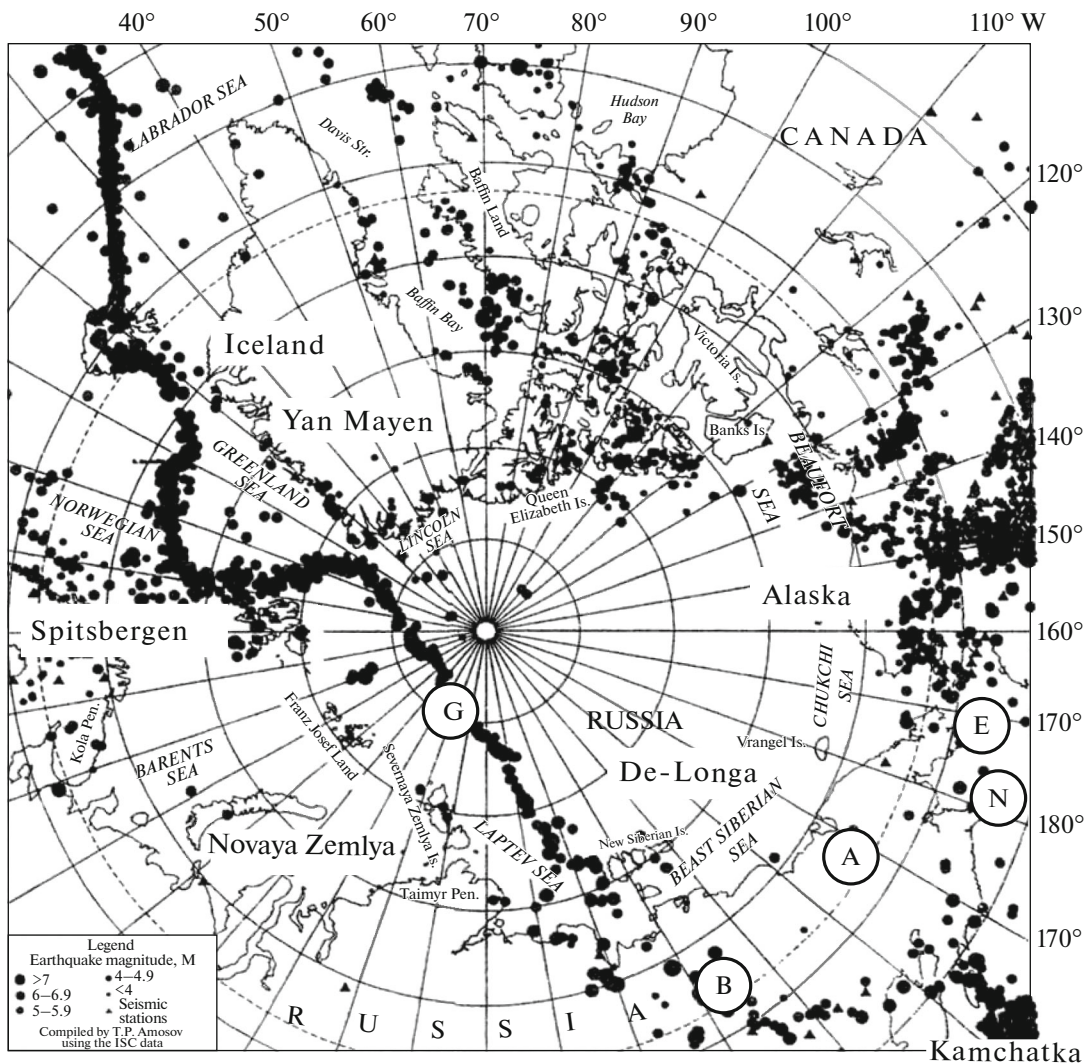


Fig. 15. (inset.)

CONCLUSIONS

The succession of large phases in eruptions of lavas and pyroclastics from Anyui Volcano is reconstructed. It is established that the volcano represented a monogenic center, while a larger share of lavas erupted from bocche located near the cone. The isotopic-geochemical composition of rocks erupted from Anyui Volcano implies their formation through partial melting in the isotopically (Nd–Sr) depleted source enriched in incompatible elements and with some contribution of the crustal contamination. Close values of ages, as well as similar petrochemical and isotopic characteristics, of Anyui and Aluchin volcanoes imply likely a single mechanism of magma generation in feeding chambers.

It is established that the radiometric age of Anyui Volcano eruption is  $0.248 \pm 0.030$  Ma. Comparison of age estimates for Anyui, Aluchin, and Balagan Tas volcanoes and young volcanics from the De-Longa Archipelago revealed the last episode of volcanism

activation in northeastern Russia (0.2–0.5 Ma ago) including its continental part (0.2–0.3 Ma ago). Activation of volcanism along the entire periphery of the Arctic and Subarctic regions is documented at the same chronological interval.

The absence of indications of the glacial abrasion on lavas from Anyui Volcano gives reasons for assuming that no significant (shield) glaciations existed in continental areas of western Chukotka at least during the last 250 ka.

The accomplished investigation revealed an insufficient knowledge of young volcanism in northeastern Russia. In this connection, a detailed petrochemical study of lavas and pyroclastics should be carried out both for Anyui Volcano proper and neighboring Aluchin and Bilibin volcanoes. The results can make it possible to determine more correctly the succession of explosive–effusive stages and reconstruct the evolution of magma during eruptions in these extremely interesting geological areas of Chukotka.

## ACKNOWLEDGMENTS

We are grateful to O.A. Shilovtseva, S.A. Orlov, and V.N. Nedostup for their help during field investigations; A.V. Lander and M.I. Tuchkova for samples for this study; S.M. Katkov for the photos; and A.A. Ariskin, A.D. Babinskii, A.O. Volynets, A.R. Heptner, A.V. Giris, O.Yu. Glushkova, V.N. Smirnov, V.V. Yarmolyuk, and Prof. Gerhard Werner for valuable recommendations during preparation of the manuscript for publishing and support of our investigations.

This work was conducted in accordance with the State contract of GIN RAS no. 0135-2014-0068 "Radiometric Chronology of Late Cenozoic Endogenic and Exogenic Events in the Russian Sector of the Arctic, Far East Region, and Adjacent Areas" and Sub-program 1 of GIN RAN within the Program no. II.3P of Presidium of the Russian Academy of Sciences. It was supported by the Russian Foundation for Basic Research, project nos. 08-05-00932 and 14-05-00549.

## REFERENCES

- Akinin, V.V. and Calvert, E., The  $^{40}\text{Ar}/^{39}\text{Ar}$  age of the Anyui volcanoes, Arctic Chukotka, in *Geokhronometricheskie izotopnye sistemy, metody ikh izucheniya, khronologiya geologicheskikh protsessov* (Geochronometric Isotope Systems, Methods for Their Study, and Chronology of Geological Processes), Moscow: IGEM RAN, 2012, pp. 25–26.
- Akinin, V.V., Evdokimov, A.N., Korago, E.A., and Stupak, F.M., Recent volcanism at the Arctic margin of North Eurasia, in *Izmenenie okruzhayushchei sredy i klimata: prirodnye i svyazannye s nimi tekhnogennye katastrofy* (Environment and Climate Change: Natural and Associated Technogenic Catastrophes), Laverov, N.P., Ed., Moscow: IGEM RAN, 2008, pp. 41–80.
- Avetisov, G.P., Tectonic factors of the intraplate seismicity in the western sector of the Arctic, *Fiz. Zemli*, 1996, no. 12, pp. 59–71.
- Bazarova, T.Yu. and Vavilov, M.A., Physicochemical conditions for the crystallization of basalt from the Anyui Volcano, *Geol. Geofiz.*, 1989, no. 2, pp. 46–50.
- Bogdanovskii, O.G., Mineev, S.D., Assonov, S.A., et al., Magmatism in the De-Longa Archipelago (Eastern Arctic): Isotope Geochemistry and Geochronology, *Geokhimiya*, 1992, no. 1, pp. 47–55.
- Bol'shoe treshchinnoe Tolbachinskoe izverzhenie (1975–1976 gg., Kamchatka)* (the Great Fissure Tolbachik Eruption of 1975–1976, Kamchatka), Moscow: Nauka, 1984.
- Bradley, R.S., *Quaternary Paleoclimatology. Methods of Paleoclimatic Reconstructions*, Boston: Allen & Unwin, 1985.
- Braitseva, O.A., Egorova, I.A., Nesmachnyi, I.A., et al., Tephrochronological studies as a method for studying regularities in the cyclic evolution of volcano, *Byull. Vulkanol. Stantsii*, 1978a, no. 54, pp. 41–53.
- Braitseva, O.A., Egorova, I.A., Nesmachnyi, I.A., et al., Tephrochronological dating of lava complexes and reconstruction of the recent volcano evolution, *Byull. Vulkanol. Stantsii*, 1978b, no. 55, pp. 41–54.
- Bronk Ramsey, C., *OxCal Program. Version 3.10. 2005.* <http://c14.arch.ox.ac.uk/oxcal3/oxcal.htm>
- Carracedo, J.C., Badiola, E.R., and Soler, V., The 1730–1736 eruption of Lanzarote, Canary Islands: a long, high-magnitude basaltic fissure eruption, *J. Volcan. Geotherm. Res.*, 1992, vol. 53, pp. 239–250.
- Cassignol, C. and Gillot, P.-Y., Range and effectiveness of unspiked potassium-argon dating: experimental ground-work and applications in *Numerical Dating and Stratigraphy*, Odin, G.S., Ed., N.Y.: John Wiley & Sons, 1982, pp. 159–179.
- Chasovitin, M.D., Quaternary volcanoes in the Kolyma region of Asia, *Tr. Irkut. Politekhn. Inst.*, 1966, no. 30, pp. 34–47.
- Chernyshev, I.V., Lebedev, V.A., and Arakelyants, M.M., K-Ar dating of Quaternary volcanic rocks: the methodology and interpretation of results, *Petrology*, 2006, vol. 14, no. 1, pp. 69–89.
- Clague, D.A., Hawaiian alkaline volcanism, in *Alkaline Igneous Rocks*, Fitton, J.G. and Upton, B.G.J., Eds., *Geol. Soc. Spec. Publ.*, 1987, no. 30, pp. 227–252.
- Dinamika landshaftnykh komponentov i vnutrennikh morskikh basseinov Severnoi Evrazii za poslednie 130000 let. Razvitie landshaftov i klimata Severnoi Evrazii* (Dynamics of Landscape Components and Inland Marine Basins in North Eurasia in the Last 130 000 Years: Evolution of Landscapes and Climate in North Eurasia), Velichko, A.A., Ed., Moscow: GEOS, 2002.
- Dobretsov, N.L., Vernikovskii, V.A., Karyakin, Yu.V., et al., The Mesozoic–Cenozoic volcanism and stages of geodynamic evolution in the central and eastern Arctic, *Geol. Geofiz.*, 2013, vol. 54, no. 8, pp. 1126–1144.
- Dovgal, Yu.M. and Chasovitin, M.D., The Bilibin Volcano: A new Quaternary volcano in the northeastern Kolyma region, *Geol. Geofiz.*, 1965, no. 6, pp. 35–46.
- Edwards, B.R. and Russell, J.K., Distribution, nature, and origin of Neogene–Quaternary magmatism in the northern Cordilleran volcanic province, *Canada GSA Bulletin*, 2000, vol. 112, no. 8, pp. 1280–1295.
- Elias, S.A. and Brigham-Grette, J., Late Pleistocene glacial events in Beringia, in *Encyclopedia of Quaternary Science*, Elias, S.A., Ed., Amsterdam: Elsevier, 2013, pp. 191–201.
- Evensen, N.M., Hamilion, P.J., and O'Nions, R.K., Rare earth abundances in chondritic meteorites, *Geochim. Cosmochim. Acta*, 1978, vol. 42, pp. 1199–1212.
- Fedorov, P.I., *Kainozoiskii vulkanizm v zonakh rastyazheniya na vostochnoi okraine Azii* (Cenozoic Volcanism in Stretch Zones on the Eastern Edge of Asia), Moscow: GEOS, 2006.
- Geologicheskaya karta SSSR. 1 : 200 000. Seriya Anyuisko-Chukotskaya. List Q-58-IX, X. Poyasnitel'naya zapiska* (Geological Map of the Soviet Union. Scale 1 : 200 000. Ser. Anyui–Chukotka. Sheets Q-58-IX, Q-58-X. Explanatory Note), Magadan: Sev.-Vost. Geol. Upravl., 1979.
- Glushkova, O.Yu., Morphology and paleogeography of Late Pleistocene glaciations in the NE Soviet Union, in *Pleistotsenovyie oledeneniya Vostochnoi Azii* (Pleistocene Glaciation of East Asia), Magadan: Sev.-Vost. Kompl. NII SO AN SSSR, 1984, pp. 28–42.
- Glushkova, O.Yu., Reflection of Climate rhythms in the topography of western Beringia, in *Chetvertichnye klimaty i rastitel'nost' Beringii* (Quaternary Climates and Plants in Beringia), Magadan: SVKNII DVO RAN, 1996, pp. 94–114.
- Glushkova, O.Yu., Geomorphological correlation of Late Pleistocene glacial complexes of Western and Eastern Beringia, *Quat. Sci. Rev.*, 2001, vol. 20, pp. 405–417.
- Gordeev, E.I., Murav'ev, Ya.D., Samoilenko, S.B., et al., The Fissure Tolbachik Eruption of 2012–2013; Preliminary

- results, *Dokl. Earth. Sci.*, 2013, vol. 452, no. 5, pp. 1046–1051.
- Gorodinskii, M.E., Dovgal, Yu.M., and Sterligova, V.E., Quaternary volcanism in the Bol'shoi Anyui River basin, *Magmatizm Severo-Vostoka Azii*, (Magmatism in Northeast Asia), Magadan: SVKNII, 1975, part 2, pp. 297–304.
- Grachev, A.F., Quaternary volcanism and problems of geodynamics in Northeast Asia, *Fiz. Zemli*, 1999, no. 9, pp. 19–37.
- Hamilton, C.W., Thordarson, T., and Fagents, S.A., Explosive lava-water interactions I: architecture and emplacement chronology of the volcanic rootless cone groups in the 1783–1784 Laki lava flow, Iceland, *Bull. Volcanol.*, 2010, vol. 72, pp. 449–467.
- Ignat'ev, V.A., New data on the Anyui volcano group (western Chukotka), *Tikhookean. Geol.*, 1990, no. 2, pp. 118–121.
- Ignat'ev, V.A., The structural position of Quaternary volcanoes in western Chukotka, *Vulkanol. Seismol.*, 1993, no. 6, pp. 28–37.
- Ignat'ev, V.A. and Sizykh, V.I., Upper Quaternary volcanoes in western Chukotka, *Priroda*, 1997, pp. 29–38.
- Ignat'ev, V.A. and Sizykh, V.I., Some problems in the study of the Bol'shoi Anyui neovolcanic test site, in *Problemy geologii i metallogeni Severo-Vostoka Azii na rubezhe tysyacheletii* (Problems of Geology and Metallogeny of Northeast Asia at the Turn of the Millennium), Magadan: SVKNII DVO RAN, 2001, pp. 158–160.
- Imaev, V.S., Imaeva, L.S., Koz'min, B.M., et al., Seismotectonic processes at the boundary of lithospheric plates in NE Asia and Alaska, *Tikhookean. Geol.*, 1998, vol. 17, no. 2, pp. 3–17.
- Irvine, T.N. and Baragar, W.R.A., A guide to the chemical classification on the common volcanic rocks, *Can. J. Earth Sci.*, 1971, vol. 8, p. 523.
- Ivanov, A.V., Arzhannikov, S.G., Demonterova, E.I., et al., The Zhom-Bolok Holocene volcanic field in the East Sayan Mts., Siberia, Russia: structure, style of eruptions, magma compositions, and radiocarbon dating, *Bull. Volcanol.*, 2011, vol. 73, pp. 1279–1294.
- Jackson, L.E., Huscroft C.A., Gotthardt, R., et al., Field guide: Quaternary volcanism, stratigraphy, vertebrate palaeontology, archaeology, and scenic Yukon River tour, Fort Selkirk area (NTS 115 I), Yukon Territory, *Geol. Surv. Can. Contr. Occas. Pap. Earth Sci.*, 2001, no. 3, 37 p.
- Kadik, A.A., Lukanin, O.A., and Lapin, I.V., *Fiziko-khimicheskie usloviya evolyutsii bazal'tovykh magm v pripoverkhnostnykh ochagakh* (Physicochemical Conditions of the Evolution of Basaltic Magmas in the Near-Surface Sources), Moscow: Nauka, 1990.
- Kereszturi, G. and Németh, K., Monogenetic basaltic volcanoes: Genetic classification, growth, geomorphology and degradation in *Updates in Volcanology – New Advances in Understanding Volcanic Systems*, Németh, K., Ed., Rijeka: InTech, 2012.
- Khain, V.E., Polyakova, I.D., and Filatova, N.I., Tectonics and petroleum potential of the eastern Arctic, *Geol. Geofiz.*, 2009, vol. 50, no. 4, pp. 443–460.
- Koloskov, A.V., Fedorov, P.I., Golovin, D.I., and Lya-punov, S.M., New data on the Late Cenozoic volcanism in Cape Navarin; Koryak Highland), *Dokl. Akad. Nauk*, 1992, vol. 323, no. 5, pp. 904–907.
- Korago, E.A., Evdokimov, A.N., and Stolbov, N.M., *Pozd-nemozoiskii i kainozoiskii bazitovyi magmatizm Severo-Zapada kontinental'noi okrainy Evrazii* (Late Mesozoic and Cenozoic Basic Magmatism at the Northwestern Continental Margin of Eurasia), St. Petersburg: VNIIOkeanologiya, 2010.
- Lacasse, C. and Garbe-Schoonberg, C.-D., Explosive silicic volcanism in Iceland and the Jan Mayen area during the last 6 Ma: sources and timing of major eruptions, *J. Volcanol. Geotherm. Res.*, 2001, vol. 107, pp. 113–147.
- Laukhin, S.A., Jain Zhimin, Pushkar, V.S., and Cherepanova, M.V., Late glaciation in the northern part of the Eastern Chukchi Peninsula and paleoceanography of the North Pacific, *Dokl. Earth Sci.*, 2006, vol. 411A, no. 9, pp. 1422–1426.
- Laverov, N.P., Lobkovskii, L.I., Kononov, M.V., et al., A geodynamic model of evolution of the Arctic basin and adjacent territories in the Mesozoic and Cenozoic and the outer limit of the Russian continental shelf, *Geotectonics*, 2013, no. 1, pp. 1–30.
- Leier, P., Parfenov, L.M., Surnin, A.A., and Timofeev, V.F., The first  $^{40}\text{Ar}$ - $^{39}\text{Ar}$  datings of magmatic and metamorphic rocks from the Verkhoyansk–Kolyma mesozoids, *Dokl. Akad. Nauk*, 1993, vol. 329, no. 5, pp. 621–624.
- Le Bas, M.J., Le Maitre, R.W., Streckeisen, A., and Zanettin, B., A chemical classification of volcanic rocks based on the total alkali-silica diagram, *J. Petrol.*, 1986, vol. 27, pp. 745–750.
- Lowe, D.J., Tephrochronology and its application: A review, *Quat. Geochron.*, 2011, vol. 6, pp. 107–153.
- Lozhkin, A.V., Anderson, P.M., Matrosova, T.V., et al., Continuous record of environmental changes in Chukotka during the last 350 thousand years, *Russ. J. Pac. Geol.*, 2007, vol. 26, no. 6, pp. 550–555.
- Mazarovich, A.O. and Sokolov, S.Yu., Tectonic subdivision of the Chukchi and East Siberian seas, *Russ. J. Earth Sci.*, 2003, vol. 5, no. 3, pp. 185–202.
- Melles, M., Brigham-Grette, J., Minyuk, P.S., et al., 2.8 million years of arctic climate change from Lake El'gygytyn, NE Russia, *Science*, 2012, vol. 337, pp. 315–320.
- Miller, E.L., Katkov, S.M., Strickland, A., et al., Geochronology and thermochronology of Cretaceous plutons and metamorphic country rocks, Anyui–Chukotka fold belt, North East Arctic Russia, in Stephan Mueller Spec. Publ. Ser., 2009, V. 4, pp. 157–175.
- Moll-Stalcup, E.J., Latest Cretaceous and Cenozoic magmatism in mainland Alaska, in *The Geology of North America*, Boulder: *Geol. Soc. Am.*, 1994, vol. G-1, pp. 589–619.
- Mukasa, S.B., Fisher, G.M., and Barr, S.M., The character of the subcontinental mantle in Southeast Asia: evidence from isotopic and elemental compositions of extension-related Cenozoic basalts in Thailand, in *Earth Processes: Reading the Isotopic Code* (Geophys. Monogr. Ser.), Basu, A. and Hart, S., Eds., Washington: AGU, 1996, vol. 95, pp. 233–252.
- Mukasa, S.B., Andronikov, A.V., and Hall, C.M.,  $^{40}\text{Ar}$ / $^{39}\text{Ar}$  chronology and eruption rates of Cenozoic volcanism in the eastern Bering Sea volcanic province, Alaska, *J. Geophys. Res.*, 2007, vol. 112, no. 18. doi 10.1029/2006JB004452
- Okrugin, A.V. and Mokhnachevskii, G.V., Structure and compositional evolution of trachybasalt flows of the Anyui Volcano in Northeast Russia, in *Geologiya i mineral'no-syr'evye resursy Severo-Vostoka Rossii* (Geology and Mineral Resources of Northeast Russia), Yakutsk: IPK SVFU, 2013, vol. 2, pp. 60–64.

- Pevzner, M.M., *Golotsenoyi vulkanizm Sredinnogo khrebtta Kamchatki* (Holocene Volcanism in the Sredinnyi Range of Kamchatka), Moscow: GEOS, 2015.
- Pevzner, M.M., Gertsev, D.O., Romanenko, F.A., and Kushcheva, Yu.V., The first data on isotopic age of Anyui Volcano (Chukotka), *Dokl. Earth. Sci.*, 2011, vol. 438, Part 2, pp. 736–738.
- Plenier, G., Valet, J.-P., Guérin, G., et al., Origin and age of the directions recorded during the Laschamp event in the Chaîne des Puys (France), *Earth Planet. Sci. Lett.*, 2007, vol. 259, pp. 414–431.
- Poyasnitel'naya zapiska k karte chetvertichnykh obrazovaniy territorii Rossiiskoi Federatsii. Masshtab 1 : 250000* (Explanatory Note to the Map of Quaternary Sediments in the Russian Federation), St. Petersburg: VSEGEI, 2013.
- Prueher, L.M. and Rea, D.K., Tephrochronology of the Kamchatka-Kurile and Aleutian arcs: evidence for volcanic episodicity, *J. Volcanol. Geotherm. Res.*, 2001, vol. 106, pp. 67–84.
- Pushkar, V.S. and Cherepanova, M.V., Beringia: Impact on paleoclimates of northeast Asia and North Pacific during Last Pleistocene glaciation, *Quat. Int.*, 2011, vol. 237, pp. 32–38.
- Razvitie landshaftov i klimata Severnoi Evrazii* (Evolution of Landscapes and Climate in North Eurasia), Velichko, A.A., Ed., Moscow: Nauka, 1993.
- Rudich, K.N., The Late Quaternary Balagan Tas Volcano (NE Asia), in *Sovremennyyi vulkanizm Severo-Vostochnoi Sibiri* (Recent Volcanism in NE Siberia), Moscow: Nauka, 1964, pp. 3–44.
- Sakhno, V.G., *Pozdneozoisko-kainozoiskii kontinental'nyi vulkanizm vostochno-azii* (Late Mesozoic–Cenozoic Continental Volcanism in East Asia), Vladivostok: Dal'nauka, 2001.
- Shilo, N.A., Lozhkin, A.V., Anderson, P.M., et al., First continuous pollen record of climate and vegetation changes in the Bering Sea region for the past 300 ka, *Dokl. Earth. Sci.*, 2001, vol. 376, no. 2, pp. 19–22.
- Singer, B.S., Guillou, H., Jicha, B.R., et al.,  $^{40}\text{Ar}/^{39}\text{Ar}$ , K-Ar and  $^{230}\text{Th}/^{238}\text{U}$  dating of the Laschamp excursion: A radioisotopic tiepoint for ice core and climate chronologies, *Earth Planet. Sci. Lett.*, 2009, vol. 286, pp. 80–88.
- Sizykh, V.I., Structural peculiarities in the spatial distribution of Quaternary volcanism in western Chukotka, *Dokl. Akad. Nauk*, 1993, vol. 328, no. 2, pp. 226–229.
- Sohn, R.A., Willis, C., Humphris, S., et al., Explosive volcanism on the ultraslow-spreading Gakkel ridge, Arctic Ocean, *Nature*, 2008, vol. 453, pp. 1236–1238.
- Sokolov, S.D., Tuchkova, M.I., and Bondarenko, G.E., Tectonic model of the South Anui suture and its role in the formation of structures in the East Arctic, in *Stroenie i istoriya razvitiya litosfery* (Structure and History of Lithosphere Evolution), Moscow: Paulsen, 2010, pp. 204–227.
- Staiger, R.H. and Jager, H., Subcommittee on geochronology: convention on the use of decay constants in geo- and cosmochronology, *Earth Planet. Sci. Lett.*, 1977, vol. 36, no. 3, pp. 359–362.
- Stratigraficheskii kodeks Rossii* (Stratigraphic Codex of Russia), St. Petersburg: VSEGEI, 2006.
- Sun, S.S. and McDonough, W.F., Chemical and isotopic systematic of oceanic basalts, in *Magmatism in Ocean Basin* (Geol. Soc., Spec. Publ.), Saunders, A.D. and Norry, M.J., Eds., 1989, vol. 42, pp. 313–345.
- Surnin, A.A., Cenozoic volcanism in NE Yakutia, in *Geologicheskoe Stroenie i poleznye iskopaemye Respubliki Sakha (Yakutiya)* (Geology and Mineral Resources in the Republic of Sakha, Yakutia), Yakutsk, 1997, vol. 2, pp. 17–19.
- Surnin, A.A., Okrugin, A.V., and Zaitsev, A.I., Deep xenoliths in basalts of eastern Yakutia, *Otechestv. Geol.*, 1998, vol. 6, no. 44, pp. 44–48.
- The 2016 Version of the International Stratigraphic Chart*. <http://www.stratigraphy.org/ICSchart/ChronostratChart2016-04.jpg>
- Thorarinsson, S., The crater groups in Iceland, *Bull. Volc.*, 1953, vol. 2, pp. 1–44.
- Thordarson, T. and Self, S., The Laki (Skaftar Fires) and Grimsvotn eruptions in 1783–1785, *Bull. Volc.*, 1993, vol. 55, pp. 233–263.
- Thordarson, T. and Larsen, G., Volcanism in Iceland in historical time: Volcano types, eruption styles and eruptive history, *J. Geodyn.*, 2007, vol. 43, pp. 118–152.
- Thordarson, T. and Hoskuldsson, A., Postglacial eruptions in Iceland, *Jökull J.*, 2008, vol. 58, pp. 197–228.
- Ustiev, E.K., The Anyui Volcano and problems of Quaternary volcanism in the NE Soviet Union, *Problemy Severa*, 1958a, no. 1, pp. 85–96.
- Ustiev, E.K., Late Quaternary volcanism in the South Anyui Range and the East Asian volcanic province, in *Molodoi vulkanizm SSSR* (Young Volcanism in the Soviet Union), Moscow: AN SSSR, 1958b, pp. 212–232.
- Ustiev, E.K., *Anyuiskii vulkan (Anyui Volcano)*, Moscow: Gosgeoltekhizdat, 1961.
- Ustiev, E.K., *Po tu storonu nochii (Beyond the Night)*, Moscow: Mysl, 1966.
- Vaganov, V.I., Ivankin, P.F., Kropotkin, P.N., et al., *Vzryvnye kol'tsevye struktury shchitov i platform* (Explosive Ring Structures in Shields and Platforms), Moscow: Nedra, 1985.
- Van den Bogaard, C., Jensen, B.J.L., Pearce, N.J.G., et al., Volcanic ash layers in Lake El'gygytyn: eight new regionally significant chronostratigraphic markers for western Beringia, *Climate of the Past*, 2014, vol. 10, pp. 1041–1062.
- Vas'kovskii, A.P., The Quaternary Balagan Tas Volcano at upper reaches of the Moma River, *Tr. Lab. Vulkanol. AN SSSR*, 1949, no. 6, pp. 3–8.
- Verkhovskaya, N.B., *Pleistotsen Chukotki* (The Pleistocene in Chukotka), Vladivostok: DNTs AN SSSR, 1986.
- Vernikovskii, V.A., Dobretsov, N.L., Metelkin, D.V., et al., Problems in the tectonics and tectonic evolution of the Arctic, *Geol. Geofiz.*, 2013, vol. 54, no. 8, pp. 1083–1107.
- Yakovlev, A.V., Bushenkova, N.A., Kulakov, I.Yu., and Dobretsov, N.L., Structure of the upper mantle in the Arctic region based on the regional seismotomography, *Geol. Geofiz.*, 2012, vol. 53, no. 10, pp. 1261–1272.
- Yarmolyuk, V.V., Nikiforov, A.V., and Ivanov, V.G., Structure, composition, sources, and mechanism of valley effusions of Zhom-Bolok lava flows (Holocene, South Baikal volcanic zone), *Vulkanol. Seismol.*, 2003, no. 5, pp. 41–59.
- Zaitsev, A.I., Surnin, A.A., and Mokhnachevskii, G.V., The strontium isotope systematics of Cenozoic basalts in NE Russia, *Otechestv. Geol.*, 2011, no. 5, pp. 64–69.
- Zigert, K., Shtaukh, G., Lemkul, F., et al., Development of glaciation on the Verkhoyansk Range and its foothills in the Pleistocene, *Regional. Geol. Metallog.*, 2007, no. 30-31, pp. 222–228.
- Zindler, A. and Hart, S., Chemical geodynamics, *Ann. Rev. Earth Planet. Sci.*, 1986, vol. 14, pp. 493–571.

Translated by I. Basov